

# Chapter 2

## Brainstem Surgery: Functional Surgical Anatomy with the Use of an Advanced Modern Intraoperative Neurophysiological Procedure



Nobuhito Morota and Vedran Deletis

### 2.1 Introduction: History of Brainstem Surgery and Intraoperative Neurophysiology

The brainstem, once called as “no man’s land,” has come to within reach of surgery by expertized hands [1–7]. Looking back at the history of brainstem surgery, the first surgical resection appeared in 1909 [8], followed by 1910 [9]. Cushing was one of those pioneers in brainstem surgery, whose first patient was operated on in 1910 with a dismal outcome [10]. Matson, one of the founders of modern pediatric neurosurgery in North America, mentioned the brainstem glioma in 1969 as “...the location of these tumors in itself obviates the possibility of surgical removal. Exploration for confirmation of the diagnosis should be avoided if possible.” However, he did not completely exclude the possibility of surgery, which was indicated only if the clinical and radiological findings were atypical [11]. On the other hand, favorable long-term outcome following surgery was reported by Pool in 1968, though all three reported patients seemed to be atypical or low-grade brainstem tumors [12]. It was not until about the early 1980s that Epstein and Hoffman used the direct surgical approach. Both of them were leading pediatric neurosurgeons at that time, fearlessly challenging the brainstem tumors [3–5, 13]. They classified brainstem tumors, mainly gliomas, and discussed surgical indications based on the tumor location and extension to the surrounding structures [3, 4, 14].

The importance of intraoperative neurophysiology (ION) arose more as direct surgical approach to the brainstem became more common and the concept of

---

N. Morota (✉)

Department of Neurosurgery, Kitasato University Hospital, Sagamihara, Japan

V. Deletis

Department of Neurosurgery, University Hospital, Zagreb, Croatia

brainstem surgery shifted from “lifesaving” brainstem surgery to “functionally preserved” brainstem surgery in the 1990s. Advanced surgical technology with detailed information of microanatomy-based surgical approaches, together with the advanced magnetic resonance imaging (MRI), opened the door to the brainstem. However, it still remained a great challenge for neurosurgeons to operate lesions in and around the brainstem. Distortion of the brainstem by a brainstem lesion leads to shifting the brainstem’s anatomical architecture. Normal landmarks which guide neurosurgeons to identify safe entry zones into the brainstem would be lost [15–19]. Brainstem auditory evoked potentials (BAEPs) have been known to reflect part of the brainstem functional integrity. It was applied as a traditional ION methodology together with somatosensory evoked potentials (SSEPs) for brainstem surgeries [20]. However, it should be reminded that the pathway of BAEPs and SSEPs covers only 20% of the brainstem area [21]. Their role in terms of preserving the functional integrity of cranial nerve motor nuclei (CNMN) is limited. A new methodology of ION for the modern use of brainstem surgery had been expected.

The dawn of ION for brainstem surgery came in 1993 when neurophysiological localization of the facial nucleus on the floor of the fourth ventricle became available and was named brainstem mapping (BSM) [22, 23]. In this original BSM, the floor was electrically stimulated using a monopolar stimulator, and the muscle response (EMG) was recorded from the targeted muscle. The muscles monitored for BSM are mainly facial (cranial motor nuclei VII: CNMN VII) and hypoglossal (cranial motor nuclei XII: CNMN XII) nuclei. Other CNMNs, such as glossopharyngeal/vagus complex (CNMN IX/X) nuclei, can be mapped in selected cases [16]. Intraoperative neurophysiological procedures can help neurosurgeons to challenge tough lesions and are expected to play a critical role in performing those demanding surgeries safely [24, 25].

This paper aims to demonstrate comprehensive clinical application of neurophysiological procedures for brainstem surgeries, focusing mainly on BSM on the floor of the fourth ventricle and the CBT-MEP monitoring [24–29]. The authors explain the detail of the surgical perspective of BSM when approached through the floor of the fourth ventricle and that of the CBT-MEP monitoring. Modified application of BSM, when approached from other skull base routes to the brainstem, is also discussed [26, 30–32]. It should be reminded that safety of surgery in and around the brainstem can be maximized with the use of those cutting-edge neurophysiological procedures.

## 2.2 Role of Intraoperative Neurophysiology

In general, ION consists of two main modalities: mapping and monitoring. The mapping technique is defined as the functional identification of nervous tissue, usually by electrical stimulation. The monitoring technique is defined as continuous feedback on the functional integrity of the nervous tissue [33]. Neurophysiological mapping in the brainstem surgery corresponds to BSM. Monitoring the motor

function integrity of CNMN corresponds to the corticobulbar tract (CBT) motor evoked potential (MEP). Combination of both mapping and monitoring is expected to enable the preservation of the functional integrity of CMN during surgery of the brainstem.

The role of ION in the brainstem surgery would be counted in three points. The first is to locate CMN on the floor of the fourth ventricle when a brainstem lesion is approached through the fourth ventricle. BSM is the answer for this purpose. The detail of BSM with its methodology and neurophysiological background is to be described later. The second is to monitor the functional integrity of the cranial nerve motor pathways originating from the cerebral cortex. The solution is the corticobulbar tract (CBT) motor evoked potential (MEP) monitoring which is emerging as an indispensable tool for the brainstem surgery [24, 29]. Neurophysiological aspects of the CBT-MEP are also described. The last is to preserve a variety of vital reflex circuits derived from the brainstem. Several new methodologies which have been introduced in the last decade are described.

### 2.3 Normal Anatomy of the Floor of the Fourth Ventricle and Safe Entry Zones

Figure 2.1 demonstrates the normal anatomy of the floor of the fourth ventricle and its subependymal intrinsic brainstem structures relating to the BSM [34, 35]. The facial colliculus and the stria medullaris are two major landmarks on the floor of the fourth ventricle. CNMN VII is mapped at the facial colliculus. It is not exactly the facial nucleus that is electrically stimulated but the intramedullary root of the facial nerve at its closest point to the floor of the fourth ventricle [18]. The stria medullaris suggests the border between the pons and medulla on the floor of the fourth ventricle. However, its direction and number have a wide individual variation; thus, it is not regarded as a reliable surgical landmark. The lower CNMNs are located beneath the hypoglossal and vagus triangles, which are included in the area of the calamus scriptorius [1, 2, 36]. CNMN XII, which locates beneath the hypoglossal triangle, is usually mapped along the midline near the obex [37]. CNMN IX/X is, if mapped, localized at the area rostro-lateral to the point where CNMN IX/X was mapped [16].

Inside of the brainstem are many vital structures and other important functions, and it is very difficult to get into its inner space safely. The term “safe entry zone” to the brainstem was first advocated by Kyoshima in 1993 [15]. Using anatomical landmarks as guidance, he demonstrated supra- and infra-facial triangles as the safe entry zone to the brainstem through the floor of the fourth ventricle (Fig. 2.1).

#### Suprafacial triangle

Medial border: the medial longitudinal fascicle (MLF)

Caudal border: the facial nerve

Lateral border: the superior and inferior cerebellar peduncles

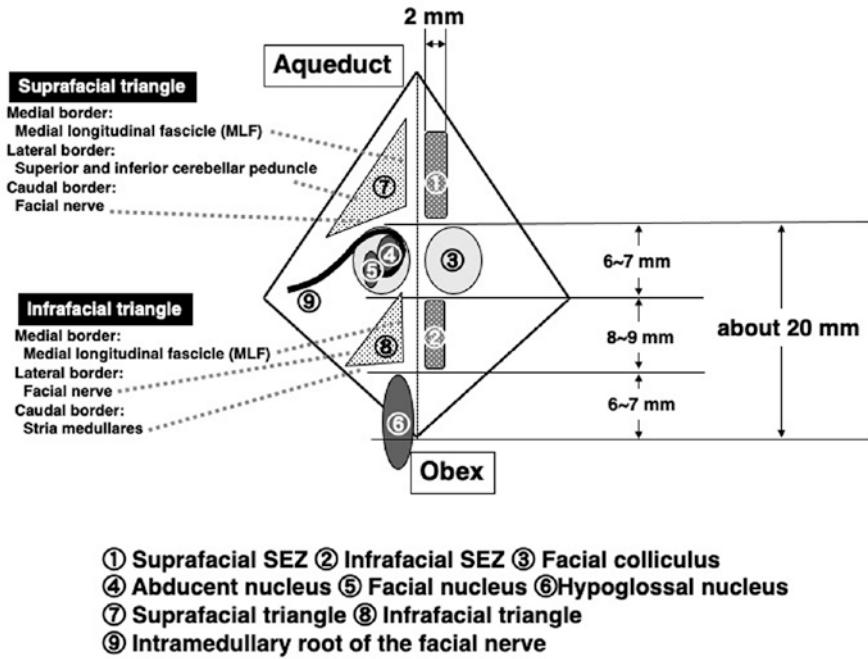


**Fig. 2.1** Normal anatomy and morphometrical measurement of the floor of the fourth ventricle. Kyoshima’s original safe entry zone on the floor of the fourth ventricle is shown in the left. The rostral end of the facial colliculus is located about 20 mm from the obex. CNMNs VI and VII locate under the facial colliculus. CNMN XII locates under the hypoglossal triangle. Note the actual SEZ is defined as more restricted area based on the morphometrical and cytoarchitectonic studies (SEZ: safe entry zone)

**Infra-facial triangle**

- Medial border: the MLF
- Caudal border: the stria medullaris
- Lateral border: the facial nerve

A series of morphometric and cytoarchitectonic studies confirmed the safe entry zone and its exact location on the floor of the fourth ventricle [37Bogucki, 18Strauss97]. The structural distance shown in Fig. 2.1 is derived from Bogucki and Strauss’s detailed morphometric anatomical study [18, 37].

The idea of “safe entry zone” to the brainstem spread and gained great applause. It ignited surgical challenge to the intrinsic brainstem lesion [1, 38]. Specific safe entry zones for other surgical approaches have been proposed since then. Bricolo added the area acustica as another safe entry zone on the floor of the fourth ventricle [2]. With the advent of skull base surgery, more than ten safe entry zones have been documented and acknowledged in the midbrain, pons, and medulla [34, 36, 38, 39].

## 2.4 Brainstem Mapping

### 2.4.1 Role of Brainstem Mapping

The original idea of BSM as an intraoperative neurophysiological procedure is to locate CNMN on the floor of the fourth ventricle (Fig. 2.2). It is the role of BSM. The original safe entry zone on the floor of the fourth ventricle under the normal anatomy does not necessarily assure safe entry to the brainstem. The brainstem is often distorted by the lesion, and the normal landmarks on the floor of the fourth ventricle would be obscure or lost [19, 22, 40, 41]. It is why BSM is required as an indispensable neurophysiological procedure to assist safe brainstem surgeries. BSM makes it possible to locate CMN on the distorted floor of the fourth ventricle and guides neurosurgeons to the area of safe entry zone to the brainstem [16, 22, 23, 27, 28].

The idea of BSM is changing as time goes on, and more surgical approaches are introduced as safe entries to the brainstem. Originally, BSM is the BSM performed on the floor of the fourth ventricle. This is a “narrow” definition. BSM on the other surface of the brainstem is relatively new [26, 30–32]. It is a contemporary application and includes more roles of the original BSM. As a “wide definition,” both original and new BSMs are included.

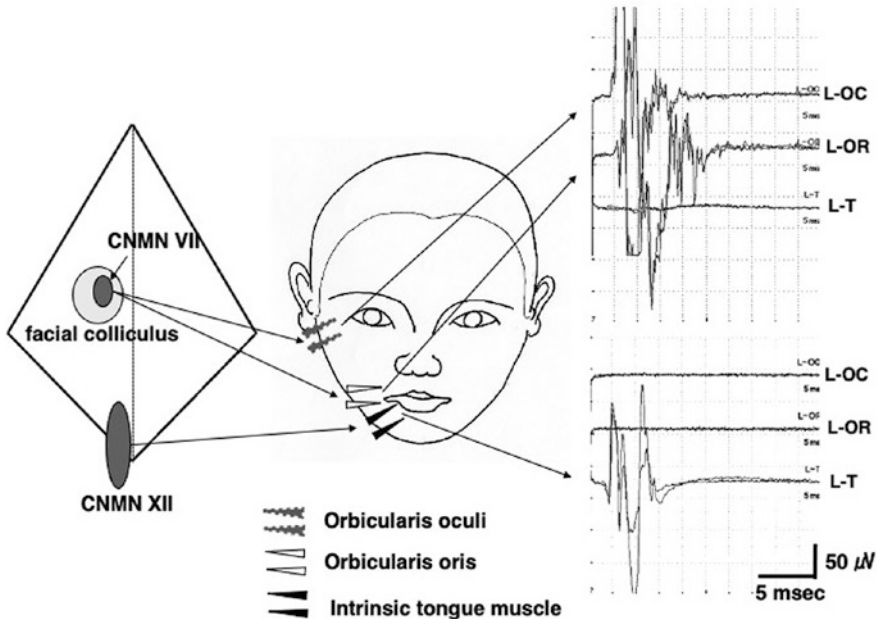


**Fig. 2.2** Schema of BSM. Left: CNMN of the floor of the fourth ventricle is electrically stimulated by a handheld monopolar stimulator. Center: A pair of EMG needles are inserted into the targeted muscles. Right: Compound muscle action potentials are recorded following the BSM of each CNMN (*L-OC* left orbicularis oculi, *L-OR* left orbicularis oris, *L-T* left intrinsic tongue muscle)

BSM enables neurosurgeons to preserve CMNs before getting into the brainstem. Direct damage to the CMN would be avoided by BSM because it tells neurosurgeons where the safe entry zone is located and how it shifts [7, 19, 27, 28, 40, 41]. It should be reminded that BSM is a mapping technique to localize a CMN and its intramedullary root. It does not reflect the functional integrity of the whole motor pathway of a CMN, including the CBT. Functional preservation of the sensory pathway is also not assured by BSM. Nevertheless, BSM plays a critical role in brainstem surgeries since functional preservation of the CMN is the primary concern for neurosurgeons who challenge the lesion inside the brainstem.

## **2.4.2 Methodology of Brainstem Mapping**

The technical aspect of BSM through the floor of the fourth ventricle has been published before, and its outline is briefly explained here [16, 28, 41].

### **2.4.2.1 Preparation for Recording**

BSM is performed through the surgically exposed floor of the fourth ventricle. Following endotracheal anesthesia, EMG electrodes are inserted into the appropriate muscles to be mapped intraoperatively (Fig. 2.2). Standard BSM for the brainstem surgery is performed for CNMNs VII and XII. A pair of EMG needles are inserted into both sides of the orbicularis oculi and oris for BSM of the CNMN VII. In the same way, a pair of EMG needles are placed into the lateral aspect of the tongue (intrinsic tongue muscle) on both sides to record the response from the CNMN XII. The impedance of the recording EMG needles should be checked before and after placing the patient in a prone position before starting surgery [16, 28, 41]. Standard recording parameters for BSM are shown in Table 2.1.

### **2.4.2.2 The Technical Aspect of Stimulation**

After surgical exposure of the floor of the fourth ventricle, electrical stimulation is delivered using a handheld monopolar stimulation probe as a cathode. The tip of the electrode is a round shape with a diameter of 0.75–1.0 mm for safety. A corkscrew electrode placed at Fz (10–20 international EEG system) or a needle electrode inserted in a muscle in the surgical field is used as a reference (anode). BSM initially starts with the stimulation intensity of 2.0 mA for searching the CNMNs. The stimulation probe on the floor of the fourth ventricle should stay at one point for a couple of seconds and move in each direction every 1 mm distance for mapping the CNMN. Once muscle responses are obtained, the stimulation intensity is gradually reduced to determine the threshold. The threshold intensity varies from 0.2 to 2.0 mA based on the relationship between the brainstem lesion and CNMNs [16, 28,

**Table 2.1** Standard parameters for BSM and CBT-MEP monitoring

	BSM	CBT-MEP monitoring
<b>Stimulation</b>		
Cathode	Handheld monopolar probe	C3(+) - C4(-) or C4(+) - C3(-)
Anode	Fz or muscles in the surgical field	Alternatively or depending on laterality of the lesion
Stimulus form	Square wave	Square wave
Stimulus duration	0.2 ms	0.5 ms
Number of stimulation	Single	Train of 5 (max. 7)
Rate	1.0–4.0 Hz	Interstimulus interval for train: 2 ms
Average	×1	Maximum intensity: 200 mA
Intensity	2.0 mA for screening, threshold intensity for precise localization	Suprathreshold intensity for monitoring
<b>Recording</b>		
Epoch time	20 ms	100 ms
Filter	20–3000 Hz	20–3000 Hz
Amplification	10,000 times	10,000 times
Muscles for EMG recording	Orbicularis oculi and oris (CNMN VII)	Orbicularis oculi and oris (CNMN VII)
	Posterior pharyngeal wall or cricothyroideus (CNMN IX/X)	Posterior pharyngeal wall or cricothyroideus (CNMN IX/X)
	Intrinsic tongue muscle (CNMN XII)	Intrinsic tongue muscle (CNMN XII)
	Other muscles innervated by CMNs as needed	Other muscles innervated by CNMNs as needed
		Abductor pollicis brevis for standard (CST-) MEP monitoring
Others	Stimulation on one point less than 5 s	No muscle response following single stimulation

41]. Minimum stimulation intensity is essential to exactly locate the CNMN [42]. Standard stimulation parameters for BSM are shown in Table 2.1. The safety of BSM under those conditions seems to be secured based on Strauss's proposal which advocated safe margin of BSM as maximum stimulation intensity of 2 mA, stimulation duration up to 400  $\mu$ s, and stimulation frequency limited to 10 Hz [19].

BSMs for CNMNs IX and X were once included as a standard BSM procedure [Morota95,96,20]. Because of the difficulty in placing electrodes, less reliability in EMG response, and obscure role in determining safe entry zone, it is no more a routine procedure in my practice. However, a new technique of recording the CNMN IX/X response from cricothyroid muscles reported by Deletis would change the clinical evaluation in the future [43]. Electrodes can also be safely inserted in the extraocular muscles for mapping CNMNs III, IV, and VI when a midbrain lesion is operated [44].

### 2.4.2.3 Anesthesia Regimen of BSM

Anesthetics used for general anesthesia have nearly no influence for BSM. Because BSM stimulates the CNMNs or the intramedullary roots, any type of anesthesia except a long-lasting muscle relaxant is compatible with BSM [16, 28, 32, 45]. However, since BSM is applied together with the CBT-MEP monitoring for the brainstem surgery, total intravenous anesthesia using propofol, fentanyl, a nitrous oxide, and oxygen mixture is the present standard anesthesia regimen. A short-acting muscle relaxant is used only before intubation.

## 2.4.3 *Functional Surgical Anatomy and Its Implications in Brainstem Surgery*

### 2.4.3.1 Functional Surgical Anatomy

Functional anatomy of the brainstem, when approached through the floor of the fourth ventricle, is revealed by BSM [19, 23, 27, 28, 40, 41]. Functional anatomy, in this situation, is nearly a synonym of surgical anatomy. Once CNMNs are mapped (positive mapping), the safe entry zone to the brainstem is identified as the silent neurophysiological area (negative mapping). The brainstem lesion is reached through the safe entry zone. BSM can be repeated from time to time on the floor of the fourth ventricle or through the lesion inside the brainstem. The advantage of BSM is that it avoids direct damage to the CNMN.

An example of functional surgical anatomy revealed by BSM is shown in the following case.

#### Case 1

This is an 11-year-old boy with diffuse intrinsic pontine glioma (DIPG). The boy showed sudden onset of consciousness disturbance with right facial weakness. Right abducens palsy and mild left hemiparesis were also presented. A CT and MRI revealed intratumoral hemorrhage of a brainstem tumor which is located in the mid-pons which predominantly shifted on the right side (Fig. 2.3). Emergency surgery for hematoma and tumor removal was carried out.

The fourth ventricle was opened through the suboccipital midline approach. The right side of the floor of the fourth ventricle was bulged by tumor and hematoma, and the median raphe shifted to the left side. BSM was performed with the stimulation intensity of 2.0 mA for a search of the CNMN (Fig. 2.3). After roughly locating the CNMNs, the stimulation intensity was squeezed to 1.0 mA for precise localization of the CNMNs. A map of functional surgical anatomy of the floor of the fourth ventricle was made (Fig. 2.4). A myelotomy was placed on the silent (negative mapping) area, compatible with the suprafacial triangle which was unrecognizable. During hematoma and tumor removal, the CBT-MEP and CST-MEP were continuously monitored. There was no change or deterioration of the MEP responses

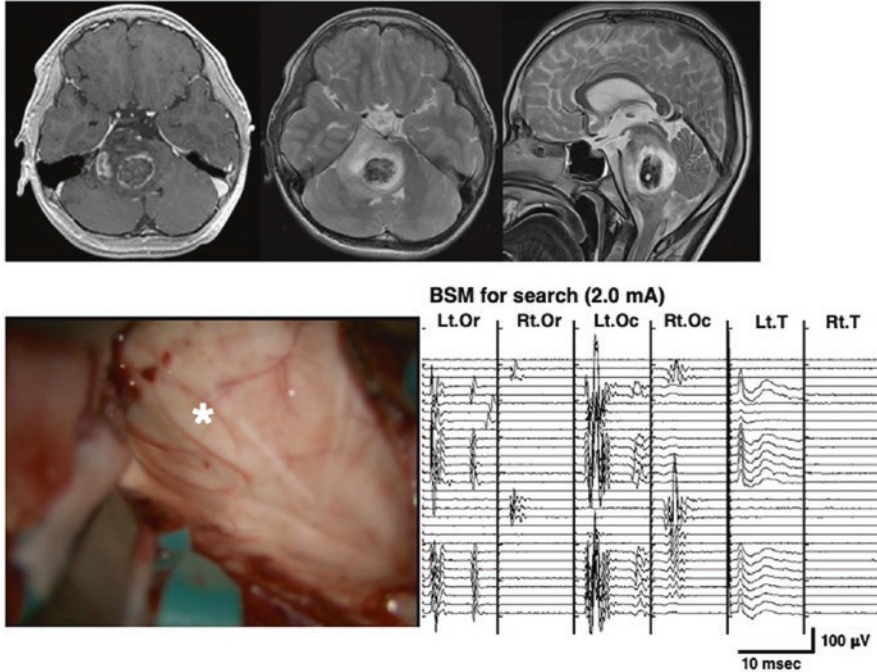


**Fig. 2.3** An 11-year-old boy with a diffuse intrinsic pontine glioma and intratumoral hemorrhage. Upper: MRI showed a diffuse intrinsic pontine tumor predominantly located in the right mid-pons with intratumoral hemorrhage. Lower left: An intraoperative photograph of the floor of the fourth ventricle showed bulging of the right side of the floor (asterisk) with a midline shift to the left side. Lower right: BSM using the stimulation intensity of 2.0 mA for a search of the CNMN (*Or* orbicularis oris muscle, *Oc* orbicularis oculi muscle, *T* intrinsic tongue muscle)

(Fig. 2.5). At the end of the hematoma and tumor removal, BSM was repeated (Fig. 2.6). Postoperatively, the boy woke up without neurological deterioration. The pathological diagnosis of the tumor was anaplastic astrocytoma.

#### 2.4.3.2 Deviation of CNMNs Caused by Brainstem Lesions

BSM demonstrated high variability in size and location of CNMN in those with brainstem pathologies [40, 41]. In our experience, BSM showed there was a repetitive pattern of the CNMN displacement depending on the location of the lesion [27, 28, 41, 45] (Fig. 2.7).

In pontine tumors, the CNMN VII is displaced around the edge of the tumor on the floor of the fourth ventricle. If a tumor is at the upper part of the pons, the CNMN VII is displaced caudally and laterally. A lower pontine tumor displaces CNMN VII rostrally and laterally. In selected cases, the orbicularis oculi and oris

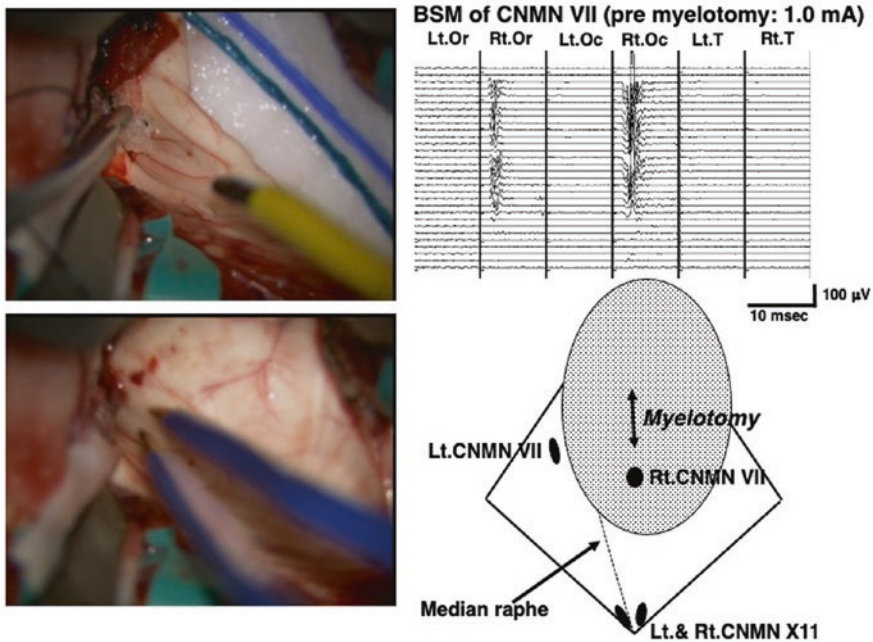


**Fig. 2.4** Upper left: BSM on the floor of the fourth ventricle, locating the CNMN VII. Upper right: BSM with the stimulation intensity of 1.0 mA for precise localization of the right CNMN VII. Lower left: Coagulation at a safe entry zone (the suprafacial triangle) on the floor of the fourth ventricle before myelotomy. Lower right: A functional surgical map of the floor of the fourth ventricle based on the result of BSM. Myelotomy was placed rostral to the right CNMN VII (same patient in Fig. 2.3)

muscle responses are mapped at a different but adjacent area on the floor of the fourth ventricle [16, 41].

In case of medullary tumors, one or more lower CNMNs locate ventrally to the tumor. It means BSM of lower CNMN before tumor resection can result in negative mapping and be unable to identify the targeted CNMN. Mapping of lower CNMN in those cases is only possible near the end of tumor resection at the bottom of the tumor cavity. Therefore, unsuccessful BSM of lower CNMN suggests important information that the lower CNMNs are located ventral to the tumor.

Although cervicomedullary junction (CMJ) spinal cord tumors are not a part of a brainstem lesion, they usually displace lower CNMN rostrally if the tumor is not a malignant invasive one [41].

It should be reminded that the abovementioned specific displacement patterns were derived from the case with a brainstem tumor. The result can be different in the case of a hematoma, cavernous angioma, and other pathologies [27, 41].

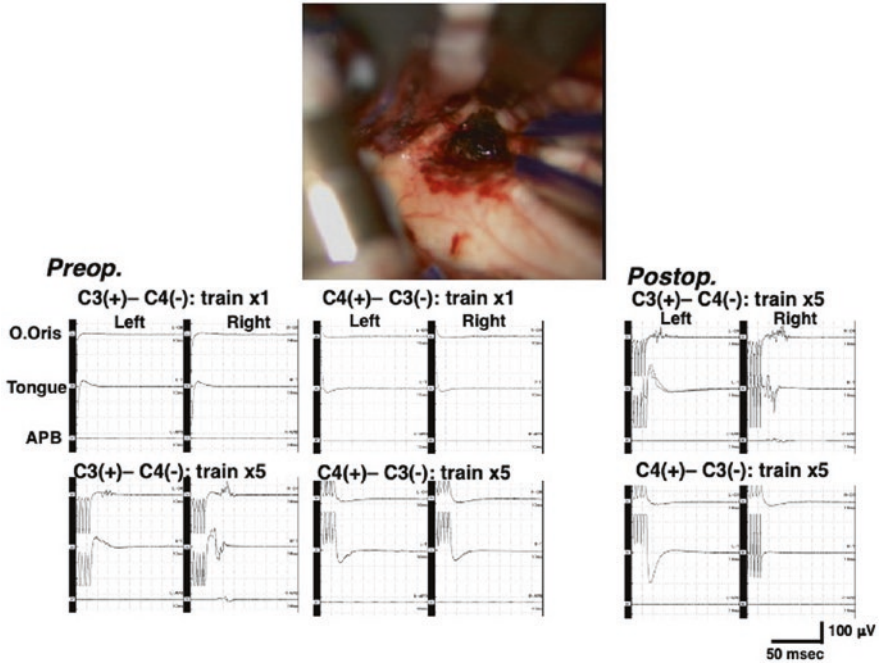


**Fig. 2.5** Upper: Removal of tumor and hematoma through the myelotomy placed on the safe entry zone (the suprafacial triangle). Lower: Recording of pre- and postoperative CBT-MEPs (stimulation intensity: 80 mA). No CBT-MEP was recorded when a single transcranial stimulation was delivered. The CBT-MEP was recorded from the left orbicularis oris muscle (O oris) and the tongue intrinsic muscle (tongue) when anodal stimulation was delivered at the C3 with a train of five stimuli (interstimulus interval: 2 ms). Small amplitude of CST-MEP was also recorded from the right abductor pollicis brevis muscle (APB). No muscle activity was evoked when stimulated from the C4. The finding was approximately the same between pre- and postoperative recordings (same patient in Figs. 2.3 and 2.4)

### 2.4.3.3 The Surgical Implication of Brainstem Mapping

BSM results on the floor of the fourth ventricle suggest several important surgical implications in terms of safe brainstem surgery [27, 28, 41, 45]. First, the risk of damaging CNMN VII exists at the edge of the tumor (Fig. 2.7). The intrinsic pontine tumor usually pushes the CNMN VII around the tumor edge. It means precise localization of the CNMN VII before tumor resection is mandatory to avoid direct damage by retraction or myelotomy incision on the floor of the fourth ventricle. Once a shifted CNMN VII is mapped, one can estimate the approximate area of the safe entry zone. In general, the midline upper pontine tumor displaces the CNMN VII caudally; thus, the safe entry zone where myelotomy is placed locates rostral to the tumor. Myelotomy should be directed rostrally. On the contrary, the midline lower pontine tumor displaces the CNMN VII rostrally; thus, the safe entry zone locates caudal to the tumor. Myelotomy should be directed caudally (Fig. 2.8).

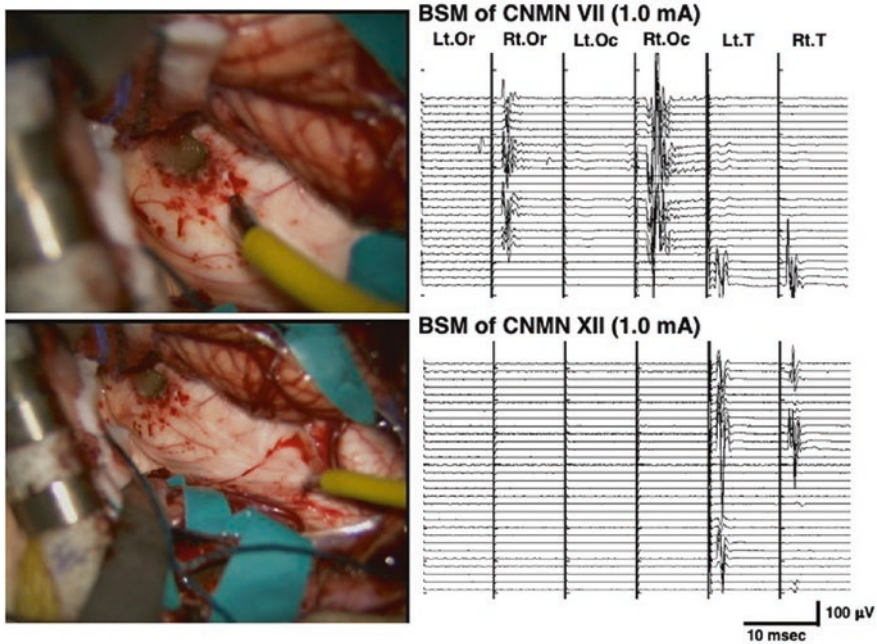


**Fig. 2.6** BSM performed after the tumor and hematoma removal. Upper: BSM of the right CNMN VII, which was located caudal to the myelotomy. Lower: BSM of the CNMN XII, which was located near the obex of the fourth ventricle (same patient in Figs. 2.3, 2.4, and 2.5)

Second, in case of the medullary tumor, the risk of damaging lower CNMN exists at the bottom of the tumor cavity (Fig. 2.8). Most tumors grow exophytic while compressing some of the lower CNMN ventral to the tumor (Fig. 2.7). Ventrally displaced lower CNMN can be unmapped before tumor resection because the tumor is on the way of stimulating current. The EMG response can appear as the tumor resection progresses to the bottom of the tumor cavity. Initial negative mapping in BSM before tumor resection is an alarming signal that the lower CNMNs are pushed ventral to the tumor. Negative mapping can turn to positive mapping on the way of tumor resection. Repeating BSM from time to time is recommended as tumor resection comes close to the bottom of the cavity. Once the unmapped lower CNMN is detected, it would be recommended to leave the rest of the tumor untouched for functional preservation of the lower CNMN (Fig. 2.8).

In the case of the CMJ spinal cord tumor, if it is large and extends into the fourth ventricle, the displacement pattern is different. The tumor pushes the caudal part of the floor of the fourth ventricle including the lower CNMN rostrally [Morota96,06,20] (Fig. 2.7). Those lower CNMNs are at high risk of damage if approached from the rostral direction. It is strongly recommended to approach the rostral end of the tumor from the caudal side while undermining the floor of the fourth ventricle (Fig. 2.8).

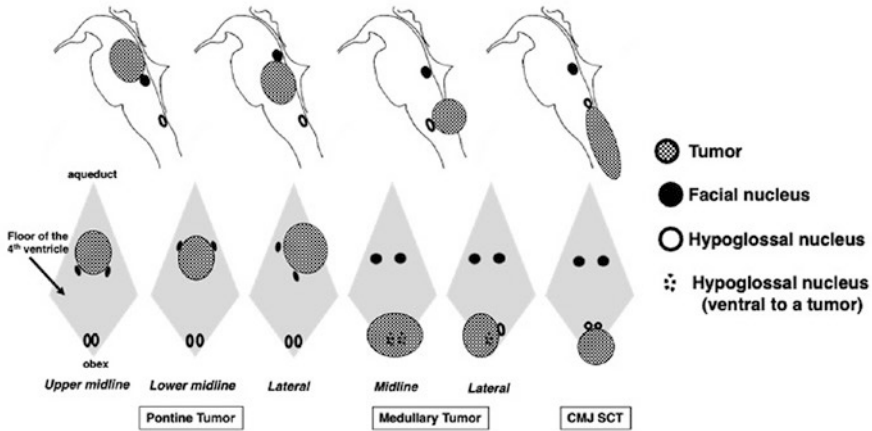


**Fig. 2.7** Typical displacement pattern of CNMN by brainstem tumors in a different location. In pontine tumors, CNMN VII is displaced at around the edge of the tumor. Precise localization of CNMN VII by BSM before tumor resection is strongly recommended to avoid direct damage during surgery. Medullary tumors typically grow more exophytic fashion. Uni- or bilateral CNMN XII could be compressed ventral side of the tumor. Failed BSM of CNMN XII before tumor resection would suggest the CMN locates at the bottom of the tumor cavity. It is recommended to repeat BSM when the tumor resection approaches near the bottom of the tumor cavity. Cervicomedullary junction spinal cord tumors (CMJ SCT) displace the lower CNMN rostrally, while the tumor extends and undermines the floor of the fourth ventricle. Care should be paid to the rostral end of the tumor cavity

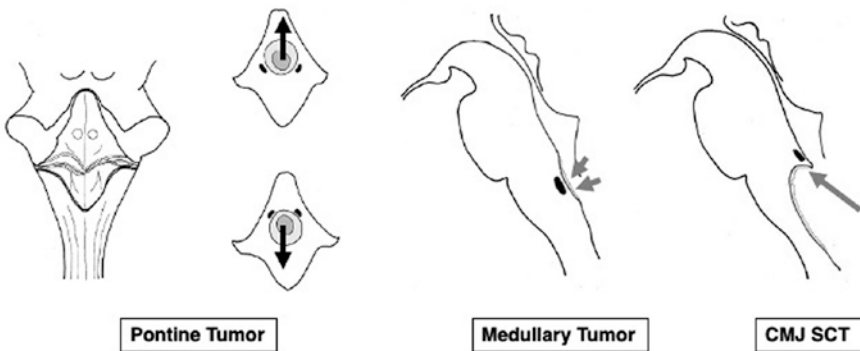


**Fig. 2.8** Surgical implications derived from BSM. Left: The midline upper pontine tumor displaces the CNMN VII caudally. Myelotomy from the exposed tumor or the shortest distance from the tumor should be directed rostrally. The midline lower pontine tumor displaces the CNMN VII rostrally. Myelotomy should be directed caudally. Center: In the case of the medullary tumor, the risk of damaging lower CNMN exists at the bottom of the tumor cavity. It is recommended to repeat BSM as tumor resection comes close to the bottom of tumor resection. Right: In the case of the CMJ spinal cord tumor, the tumor pushes the caudal part of the floor of the fourth ventricle rostrally. The risk of damaging the lower CNMN exists at the rostral end of the tumor

#### **2.4.4 *Limitations of Brainstem Mapping***

BSM has been recognized as an indispensable intraoperative neurophysiological procedure that protects the CNMN from direct damage during surgery of brainstem lesions. Distorted brainstem anatomy fails to indicate the exact location of displaced CNMN. Positive BSM outlines the dangerous area to enter the brainstem. Negative BSM suggests a relatively safe entry zone to the brainstem. Without BSM, a neurosurgeon would be at a loss to find safe entry zone to get into the brainstem lesion. However, BSM does have limitations.

First, BSM is a neurophysiological mapping technique, not a monitoring one. BSM is performed intermittently to localize the CNMN or confirm the functional integrity distal to the CNMN. It is not a continuous procedure to monitor the functional integrity of the CNMN throughout the surgery. When performed, surgery must be interrupted. In addition, repeating BSM frequently consumes time. Nevertheless, damage to the CNMN can develop during the tumor resection between BSMs. To overcome this limitation, combined use of BSM and the CBT-MEP monitoring is strongly required [24, 27, 29].

Second, BSM cannot detect or prevent direct damage to the CBT. Preserved EMG response evoked by BSM does not necessarily assure preserved CBT functional integrity. Chance of selective CBT injury seems unlikely when approached from the floor of the fourth ventricle since the CBTs generally approach the CNMN from a ventral to the dorsal direction [46]. However, the possibility of CBT injury cannot be excluded completely.

Third, positive results of BSM of the lower CNMN do not necessarily guarantee preserved lower brainstem function. Functional integrity of the lower CNMN involved in swallowing, coughing, and vocalization consists of both afferent (sensory) and efferent (motor) reflex circuits. Damage to the intramedullary afferent root or inter-nucleus connecting pathway is undetectable by BSM. It should be reminded that Pick's bundle, one of the medullary CBT branches, forms a loop to innervate lower CNMN (Figs. 2.9 and 2.10). One of its roles is supposed to be connection between the lower CNMNs [46, 47]. Theoretically, damage to Pick's bundle while having positive BSM still can lead to the functional deterioration of the lower CNMN postoperatively.

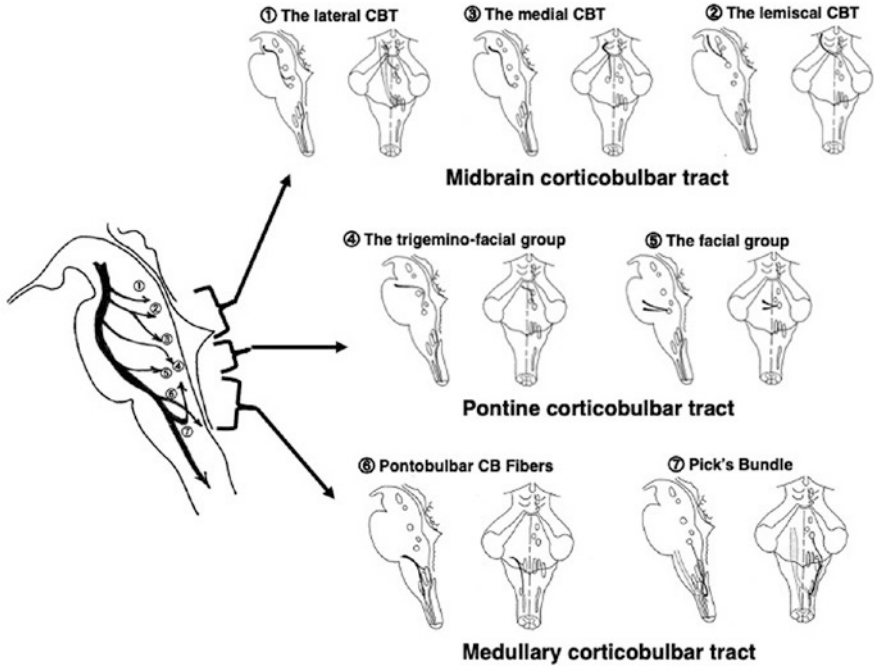


**Fig. 2.9** Schematic drawing of the CBT and its branches. The branches are classified into three groups based on the anatomical location. Note that the CBT innervates CNMN in the ventrodorsal direction with multiple innervations to a CMN (from Morota et al., Intraoperative neurophysiology for surgery in and around the brainstem: role of brainstem mapping and corticobulbar tract motor-evoked potential monitoring. *Child Nervous System*, 26, pages 513–521 (2010), with permission)

## 2.5 Corticobulbar Tract

### 2.5.1 Anatomy of CBT

There has been limited knowledge about the detailed anatomy of CBT innervating the CNMN in the brainstem. The CBT is derived from the precentral gyrus and run down aside the corticospinal tract (CST) [48]. It passes the genu of the internal capsule, medial-most region of the cerebrum peduncle, and then spreads into several branches as it goes down [49]. Several branching fibers to the CNMNs VII and XII have been depicted on recent MRI-based studies [47, 50–52].

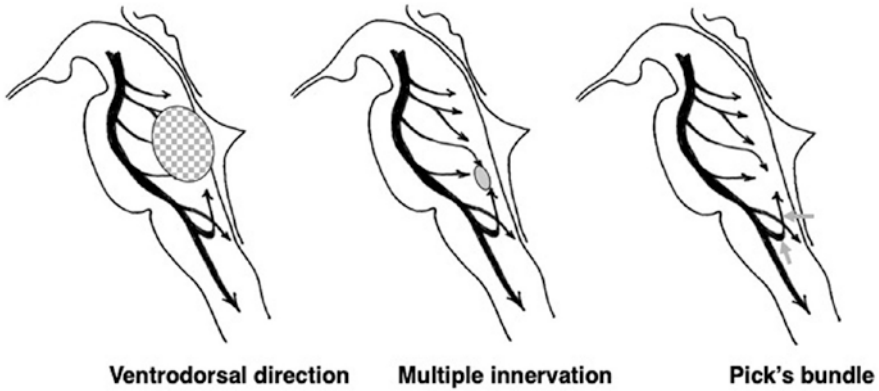


**Fig. 2.10** Surgical implications based on the CBT anatomy. Left: The CBT runs ventral-to-dorsal direction to CNMNs. Direct damage to CNMNs seems less likely if the brainstem lesion was approached from the floor of the fourth ventricle. Center: The CNMN receives several branch fibers from the CBT. Multiple innervations of the CNMN by CBT branches mean that the permanent CNMN dysfunction is less when a single branch fiber was damaged. Right: Pick's bundle (gray arrows) forms a medullary loop. Its damage would result in serious lower cranial nerve dysfunction

Krieg is the first to reveal the minute anatomy of the CBT using what we call “fiber dissecting method” in the 1950s [46]. According to his study, the CBT diverges from the CST in the brainstem as several branch fibers. His description of the CBT origin was as follows: “Fibers for the cranial nerve nuclei are the most medial of the pyramidal fibers in the peduncle, but below this level they begin to leave the peduncle to reach their terminations in the brain stem” (Fig. 2.9).

Seven main branches were described, and their courses to the CNMN were shown in a three-dimensional figure in Krieg’s book. These branch fibers were classified into three groups based on their locations and targets in the brainstem: mid-brain CBT, pontine CBT, and medullary CBT (Fig. 2.9) [24]. Each branch included two to three groups of fibers that synapse directly to the CNMN or indirectly through interneurons. The following explanations are a summary of the original Krieg’s description [46].

### Midbrain CBT

1. The lateral CBT: It separates the dorsomedial face of the peduncle, directs dorsomedially into the tegmentum, then decussates, and descends to terminate the CNMN V.
2. The medial CBT: It separates from the peduncle, curves ventromedially, then runs dorsally between the medial lemniscus fibers (MLF), turns caudally along the medial of the MLF, decussates, and passes dorsolaterally to reach the CNMN VII and possibly to the CNMNs V and VI.
3. The lemniscal CBT: It courses much like that of the medial CBT, but it diverges laterally to pass into the CNMN V and it branches laterally to pass.

### **Pontine CBT**

4. The trigemino-facial group: It leaves the pyramidal tract at dorsomedial aspect in the upper pons. It reaches the midline and courses directly dorsally just below the fourth ventricle, then decussates, goes laterally to the CNMN VI, and ends to the CNMNs V and VII.
5. The facial group: It leaves the dorsal aspect of the pyramidal tract in the middle and lower pons. After reaching the midline, it gradually decussates and runs dorsally and then runs directly to the CNMN VII.

### **Medullary CBT**

6. The pontobulbar corticobulbar fibers: It leaves the pyramidal tract at the ponto-medullary junction and runs dorsally to end in the CNMN XI and spinal accessory nuclei.
7. Pick's bundle: It leaves the pyramidal tract just after decussating, turns cranially, and runs upward just medial to the spinal ambiguous nucleus, while its highest fibers run up to the CNMN VII.

## **2.5.2 Surgical Implications of CBT Anatomy**

Krieg's detailed description of the normal anatomy of the CBT gives us information when we face the brainstem surgery (Fig. 2.10). First, the CBT is not a single bundle like the CST. It is an assembly of a group of fibers. Second, after the CBT branches leave the CST, they run ventral-to-dorsal direction to the CNMN in the brainstem. It means that if the brainstem lesion is approached from the floor of the fourth ventricle, it seems less likely to damage the CBT directly. Third, the CNMN receives several branches from the CBT. There seems to be no one-to-one innervation between a CBT branch and a CNMN. Multiple innervations of the CNMN by CBT branches mean it behaves like a biological "safeguard system," less vulnerable to damage. A single injury to a CBT branch does not necessarily result in CNMN dysfunction. Mild to moderate motor dysfunction of the CNMN caused by direct damage to a CBT branch could possibly recover later. Fourth and finally, one branch of the CBT (Pick's bundle, in the medullary CBT) forms a medullary loop and turns to run caudal-to-rostral direction while innervating the pontomedullary cranial nuclei [47, 51–53]. This atypical, unusual route of the CBT branch could have some role in the complex reflex circuits formed among the lower cranial nerves [24, 27]. Damage to Pick's bundle would cause injury to those critical reflex circuits and result in serious lower cranial nerve dysfunction.

### 2.5.3 CBT-MEP Monitoring

The functional integrity of the entire CBT ending up to the CNMN is monitored by the CBT-MEP monitoring during the surgery in and around the brainstem [24, 25, 26, 29].

In Fig. 2.11, a 2-year-old boy with anaplastic ependymoma demonstrates the optimal indication for CBT-MEP monitoring. The tumor located at the right cerebellopontine angle to a pontomedullary junction and extended to the ventral side of the brainstem. The fourth ventricle was compressed and shifted to the left side. BSM was inapplicable since the floor of the fourth ventricle would be exposed at the last stage of tumor resection. Intramedullary and subarachnoid parts of the peripheral facial and lower cranial nerves, together with the CBT, seemed to be at high risk of damage by tumor resection. The CBT-MEP monitoring plays a critical role in performing the safe tumor removal by the feedback of real-time functional integrity of the CBT to surgeons [24].

The technical aspect of the CBT-MEP monitoring has the common background in terms of placing electrodes for recording (Fig. 2.2). Stimulation electrodes are placed at C3 and C4 (10–20 international electroencephalographic electrode system) (Fig. 2.12). Using C3 and C4 electrodes alternatively as anode for transcranial electrical stimulation (TcES), the CBT-MEP on each side is recorded from the same muscles used for BSM. The parameters of TcES for the CBT-MEP are the same as the standard CST-MEP monitoring. Train of five stimuli with the interstimulus interval of 2 ms (500 Hz) is delivered over the scalp to elicit the CBT-MEP. Before monitoring the CBT-MEP, a single transcranial electrical stimulation is delivered to

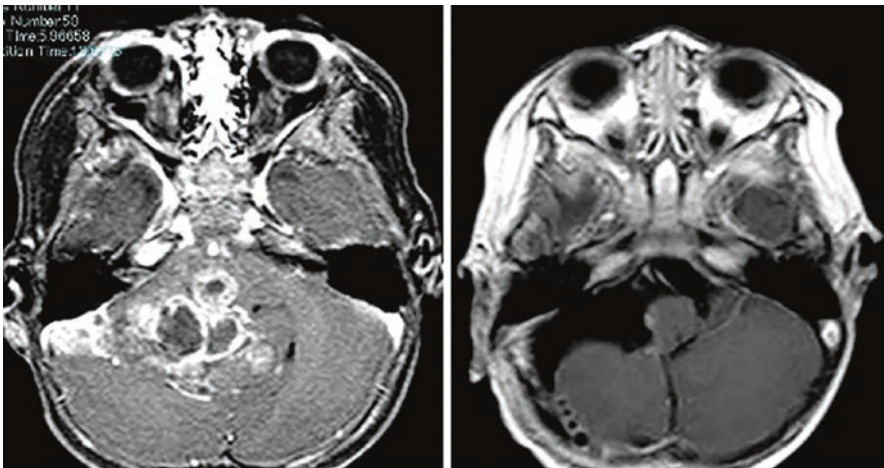


**Fig. 2.11** A case of anaplastic ependymoma in a 2-year-old boy. Left: Preoperative Gd-enhanced MRI demonstrated the tumor extending from the right cerebellopontine angle to the ventral side of the brainstem. Right: Postoperative Gd-enhanced MRI showed gross total resection of the tumor. A small part of the tumor remained on the right lateral surface of the brainstem

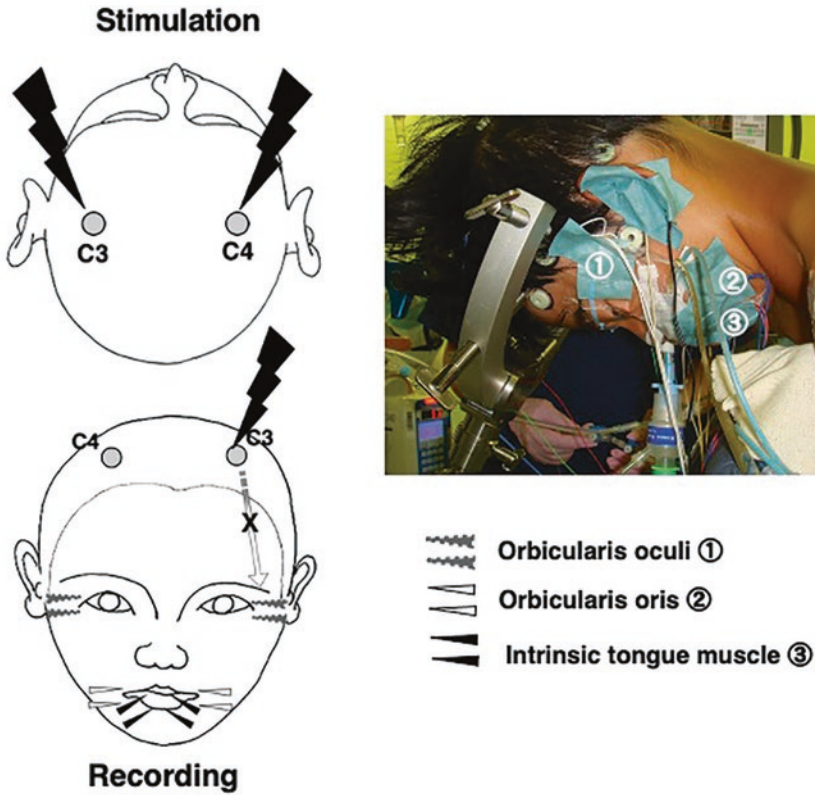


**Fig. 2.12** Left: Position of electrodes placed for transcranial stimulation of the CBT-MEP and for recording from cranial nerve-innervated muscles. Recording from the orbicularis oculi muscle is excluded whenever surface conduction of the stimulation current is suspected. Right: Intraoperative photograph after turning the patient in a prone position. Electrodes for recording are fixed on the face with tapes

confirm that the response originated from the CBT, not by peripheral activation of the facial nerve induced by surface conduction from the stimulation electrode (Fig. 2.13). If any muscle contraction is recorded following a single stimulation, the stimulation intensity is reduced to avoid the muscle contraction evoked by surface conduction of the current (Fig. 2.1). Subthreshold stimulation intensity is the must-rule for eliciting reliable CBT-MEPs. The maximum stimulation intensity is restricted up to 200 mA for safety reasons, the same as the standard CST-MEP monitoring.

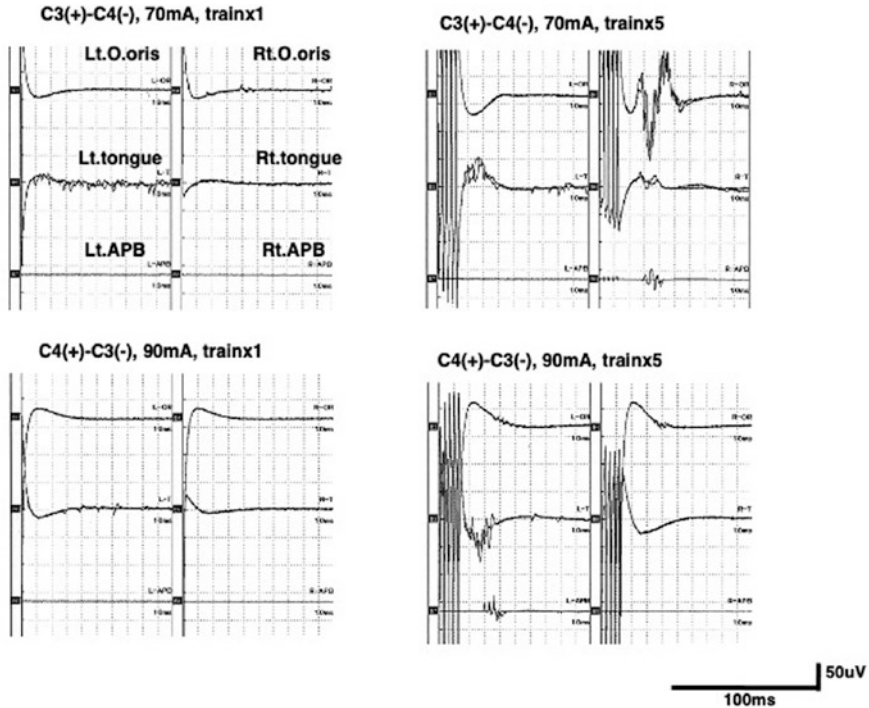


**Fig. 2.13** Record of the CBT-MEPs. Left: Prior to monitoring the CBT-MEP, no response following a single transcranial electrical stimulation is confirmed to exclude the peripheral activation of the facial nerve. Right: Train of five stimuli with the interstimulus interval of 2 ms (500 Hz) is delivered to elicit the CBT-MEP (*O oris* orbicularis oris muscle, *tongue* intrinsic tongue muscle, *APB* abductor pollicis brevis muscle)

### 2.5.4 Advantages and Limitations of Monitoring the CBT-MEP

The advantages of the CBT-MEP monitoring are that it can be applied in all surgeries in and around the brainstem [24, 43, 54]. Its clinical use during surgery of acoustic neuroma and other skull base surgeries has been reported [55–59]. In addition, the advantage of monitoring the CBT-MEP is that it enables to monitor the entire motor pathway from the motor cortex to the cranial motor nerve-innervated muscle. Unlike BSM, which interrupts surgery for the mapping, the CBT-MEP is monitored simultaneously with the surgical procedure [55].

Limitation in monitoring the CBT-MEP does exist. It has been pointed out that possibility of peripheral activation by surface conduction cannot be completely excluded entirely when monitoring the facial CBT-MEP [60]. It could lead to a false-negative result and should be avoided. Since the orbicularis oculi muscle is most vulnerable to peripheral activation caused by surface conduction, it would be excluded from the CBT-MEP monitoring in selected cases. Another limitation is its

lack of monitoring of the sensory part of the cranial nerves and their contribution to the sensory pathway. Reflex circuits of swallowing and coughing could be damaged without reflecting on the CBT-MEP monitoring. The lower cranial nerves are composed of sensory and motor parts. The CBT-MEP monitoring can monitor the functional integrity of the whole motor pathway to the CNMN but not the sensory pathways of cranial nerves. Considering the anatomical background of the CBT, it would be fair to say that the result of CBT-MEP monitoring innervating CNMNs VII and XII can correspond to functional preservation. This result may show some discrepancy for CNMN IX/X. The CBT-MEP monitoring cannot monitor sensory input through the afferent fibers. Lower cranial nerve dysfunction, such as dysphagia and dysarthria, can develop despite preserved CBT-MEP responses. Preserved CBT-MEPs do not necessarily assure the preserved lower cranial nerve function [57]. Finally, defined warning criteria for the CBT-MEP monitoring have not been established. Amplitude reduction of more than 50% has been reported, with the same warning criteria as the CST-MEP [58]. However, it should be carefully verified because it is not sure that the same criteria can be applied for pure motor function (CNMN VII, CNMN XII) and the lower CNMN included in the complex reflex circuit. Different criteria based on a different function of the CNMN could be required in the future.

## 2.6 Comprehensive ION Procedures in the Contemporary Brainstem Surgery

It should be emphasized again that the branches of CBT run ventrodorsal direction and the CMN is innervated by multiple CBT branches (Figs. 2.9 and 2.10) [17, 27, 46, 47, 50]. Those anatomical features of CBT suggest that permanent damage to the CBT is less likely when the lesion is approached from the fourth ventricle. Nevertheless, damage to the CNMN and its intra- or extramedullary root can develop during the surgery. The situation is the same when other various skull base approaches are used for the brainstem surgery [32]. It is the reason why the combined application of both BSM and the CBT-MEP monitoring is critical and indispensable for the safe surgery in and around the brainstem [24, 29, 61]. It is the role of ION procedures in contemporary brainstem surgeries.

Presently, newly recognized safe entry zones exist in almost all aspects of the brainstem surface [7, 34, 38, 39, 62]. Even if a brainstem lesion is approached other than through the floor of the fourth ventricle, the role of BSM still exists. Together with the CNMN, the CST and CBT can be mapped either positively or negatively (Fig. 2.14) [26]. Positive mapping on the brainstem surface warns that there is a critical brainstem structure present underneath the region. Negative mapping assures that the mapped site is safe to get into the brainstem.

BSM can be applied through inside of the brainstem to estimate how the mapped point is close to an intrinsic brainstem structure [63]. It is the brainstem version of

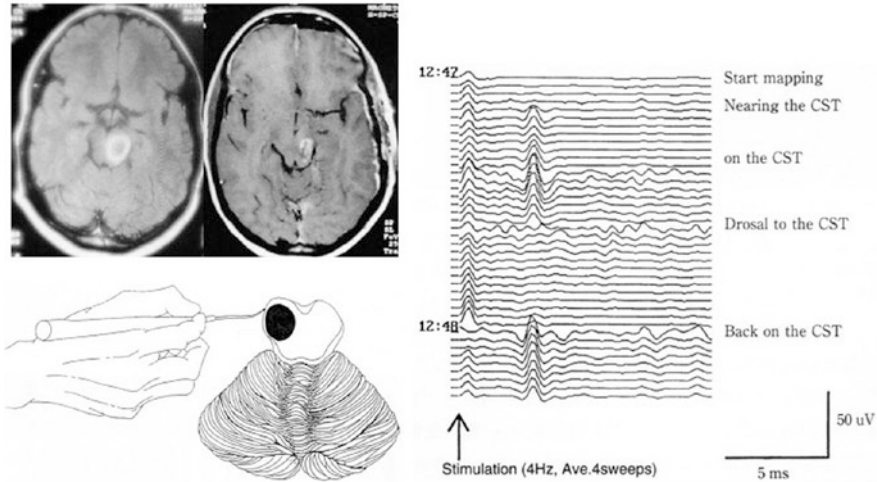


**Fig. 2.14** Modified application of BSM for detecting the CST on the lateral surface of the brainstem. The CST was mapped on the lateral surface of the midbrain. Left upper: Pre- and postoperative MRI showing subtotal removal of the left midbrain tumor. Left lower: Schematic drawing of modified application of BSM. Right: BSM on the lateral surface of the midbrain demonstrated the D waves recorded from an electrode inserted in the spinal epidural space, when the stimulation is delivered on the left CST (positive mapping). No response was recorded when the stimulation moved dorsally from the tumor (negative mapping)

the subcortical white matter mapping [64]. It should be reminded that the relationship between stimulation intensity and the distance from the point of stimulation to the mapped structure demonstrated no linear correlation [65, 66]. Variability of the estimated distance would come from a heterogeneity of tissue, the condition of the surgical field, and different neurophysiological parameters [65, 67]. It would be especially true in the brainstem where CMNs and their intramedullary roots exist together with the CBT and CST. On the other hand, from the practical viewpoint, rough estimation “1 mA = 1 mm” (stimulation of 1 mA intensity penetrates 1 mm within the brainstem tissue) is derived according to Shibani’s data [65]. This is an approximation and should be adjusted from patient to patient.

Representative cases of the brainstem surgery are presented.

## Case 2

This is a 7-year-old girl with a long history of gait disturbance and slow progression. Mild hoarseness and swallowing also gradually developed. An MRI revealed a lesion with high signal intensity on T2-weighted image from the right pons to the cerebellar peduncle (Fig. 2.15). Open tumor biopsy through the fourth ventricle was performed.

After exposure to the floor of the fourth ventricle, BSM was performed. The initial stimulation intensity of 1.0 mA was delivered to search the location of the CNMNs. Then, the stimulation intensity was reduced to 0.4 mA for precise localization of the CNMNs (Fig. 2.15).

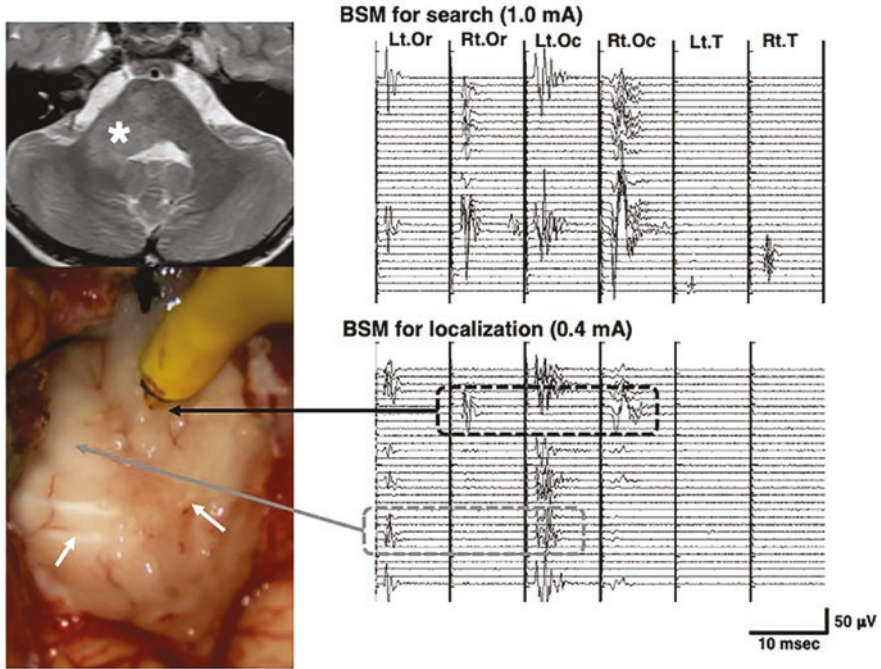


**Fig. 2.15** A 7-year-old girl with a tumor extending from the cerebellar peduncle to the brainstem. The girl presented with ataxic gait, which gradually worsened over a few years. Hoarseness and occasional swallowing difficulty developed slowly. Upper left: An MRI revealed a high signal intensity from the right cerebellar peduncle to the brainstem on T2-weighted image (asterisk), and there was no enhancement after the gadolinium injection. Upper right: BSM for search of the CNMNs with the stimulation intensity of 1.0 mA. Lower: With the use of a stimulation intensity of 0.4 mA, precise localization of the CNMN VII was performed. The black arrow indicates the right CNMN VII, and the gray arrow is the left one (white arrows: stria medullaris)

The tumor biopsy was performed near the base of the right cerebellar peduncle, away from the right CNMN of the facial nerve. The CBT-MEP remained stable before and after the biopsy, though the responses from the CNMN VII were very small in amplitude (Fig. 2.16).

To the brainstem lesion located more ventrally, the lateral approach would be the choice of surgery [34, 38, 68, 69]. Bertalanffy strongly recommended the posterolateral approach to the pons as it was safer to preserve CNMN VI and VII function than approaching through the floor of the fourth ventricle [7]. BSM can reveal the location of the CST or CNMN on the lateral surface of the pons (Fig. 2.14) [26]. The CBT-MEP monitoring is continuously carried out through the surgical approach and procedures inside the brainstem.

### Case 3

This is an 11-year-old boy with a pontine cavernous angioma. The boy had a history of repeated hemorrhage from a pontine cavernous angioma. He underwent removal

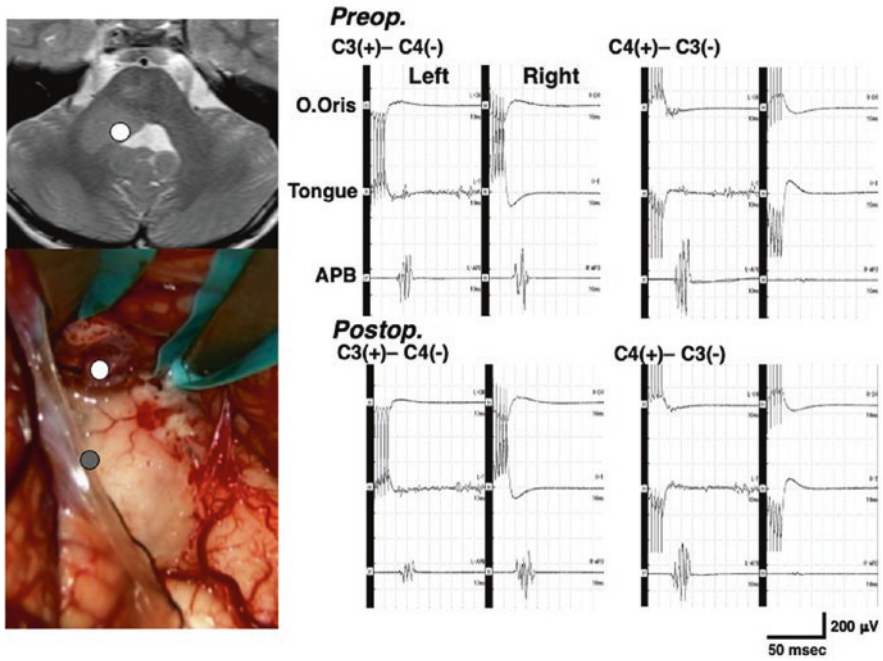


**Fig. 2.16** Upper left: A white circle shows the lesion where biopsy specimens were sampled. Lower left: Intraoperative photograph shows the biopsy taken from the white circle. A dark circle shows the location of the right CNMN VII. Right: Pre- and postoperative CBT-MEPs (stimulation intensity: 80 mA). In this case, CBT-MEPs from the left CNMNs remained stable but were absent from the right CNMNs. Note CST-MEPs recorded from the APB remained stable (same patient in Fig. 2.15)

of the cavernous angioma through the supracondylar fossa (far lateral) approach 2 years before the second surgery. The rostral part of the angioma was tightly attached to the surrounding brainstem tissue and left untouched. This time, he noticed worsened right facial palsy and right hemiparesis. A CT and MRI revealed rebreeding from the residual angioma (Fig. 2.17). The second surgery was scheduled through the posterior trans-petrosal approach. During the surgery, the lateral surface of the pons was exposed after cutting the cerebral tentorium and opening the arachnoid membrane. BSM was carried out on the lateral surface of the pons between CNMNs V and VII (Fig. 2.18). The CNMN VII was located at the caudal end of the surgical field (positive mapping). Myelotomy of the pons was placed on the silent area of BSM (negative mapping), which was supposed to be a safe entry zone of the infratrigeminal lateral approach to the pons [7, 34, 39]. The hematoma and the angioma were gross totally removed. The CBT-MEP and the CST-MEP were continuously monitored during the procedure (Fig. 2.18). The CBT-MEP of the right CNMNs VII and XII remained approximately the same amplitude. In

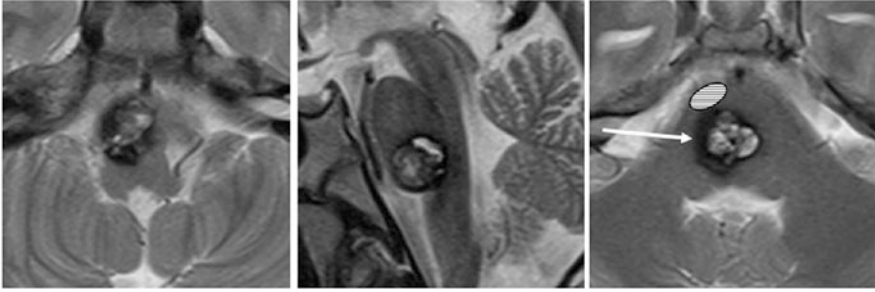


**Fig. 2.17** An 11-year-old boy with recurrent hemorrhage from a brainstem cavernous angioma. Left and center: Recurrent hemorrhage from a cavernous angioma was observed in the right lower pons. Right: Surgical approach to the pons (arrow) and the location of CST (lined oblique oval) are shown

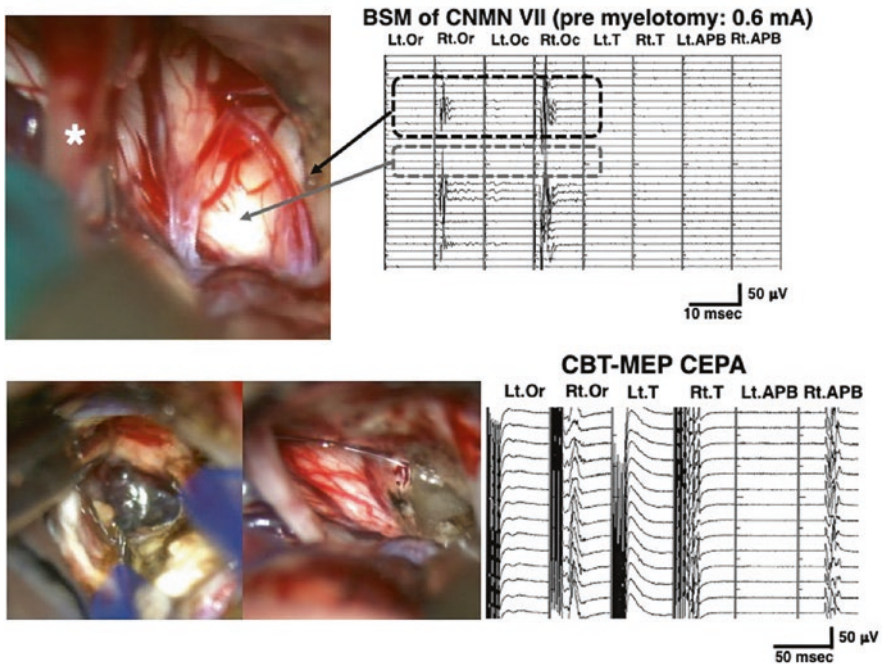


**Fig. 2.18** Upper: Result of BSM on the lateral surface of the pons. When stimulated between the trigeminal (asterisk) and facial nerves, no response was recorded (negative mapping: dark arrow). Facial muscle contraction was recorded when stimulated near the exit zone of the facial nerve (positive mapping: black arrow). Lower left and center: Exposure of the cavernous angioma (left) and after removal of the cavernous angioma (center) was shown. Lower right: The CBT-MEP and the CST-MEP were continuously monitored during the surgical resection of the cavernous angioma (CEPA, continuous evoked potential array; Or, orbicularis oris muscle; Oc, orbicularis oculi muscle; T, intrinsic tongue muscle; APB, abductor pollicis brevis muscle) (same patient in Fig. 2.16)

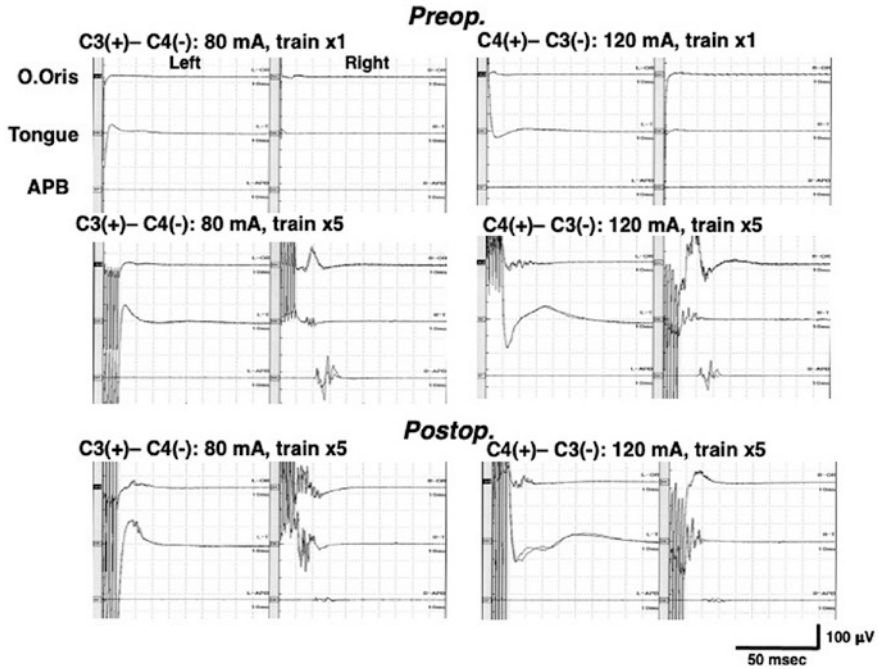


**Fig. 2.19** Pre- and postoperative recordings of the CBT-MEP. Note there was no muscle contraction when transcranial electrical stimulation was delivered by single stimulation. By the end of surgery, the CBT-MEP was approximately preserved, but the CST-MEP from the right APB reduced its amplitude (*O oris* orbicularis oris muscle, *tongue* intrinsic tongue muscle, *APB* abductor pollicis brevis muscle) (same patient in Figs. 2.16 and 2.17)

contrast, the CST-MEP on the right side reduced its amplitude (Fig. 2.19). The boy woke up with mildly deteriorated right hemiparesis, but it improved within a month.

## 2.7 Future Perspective on the Role of ION Procedures in the Brainstem Surgery

Surgery to the brainstem has made remarkable advancements in the last two decades after the introduction of various skull base approaches [70, 71]. With the advent of surgery, so were the ION procedures applied for brainstem surgical interventions. Original BSM through the floor of the fourth ventricle is no more the sole procedure of BSM in the contemporary ION.

### ***2.7.1 Advanced Brainstem Imaging and the Role of ION***

Morphometrical visualization of the brainstem to support anatomical guidance to the brainstem structure was first attempted at the end of twentieth century [72]. Presently, diffusion tensor tractography (DTT) visualizes the pyramidal tract noninvasively in the brain and has been regarded as promising technique which enhances the capability of surgical approach, mainly for brain tumors [73, 74]. The accuracy of DTT in relationship with the brain lesion still remains controversial, and the combined use of ION has been discussed [75–77]. Nevertheless, DTTs of the CST and CBT have been opening a new field of the brainstem’s functional anatomy and its surgery [52, 78, 79].

Recent advancements in MRI have brought great impact not only in diagnosis but also the selection of surgical approaches. Subnuclei in the basal ganglion can be visualized by using 7 T MRI [80]. Furthermore, the presently invisible internal architecture of the brainstem can be visualized using 11.7 T MRI [62]. An anatomical safe entry zone to an intrinsic brainstem lesion can be defined on an 11.7 T MRI before surgery.

It would be possible to reach the lesion with the use of a high-resolution MRI-guided navigation system. If DTT of the CBT has reached the clinical use, it would also be helpful for the surgeon to plan a surgical approach. It means an “on the image” safe entry zone can be visualized with high-resolution MRI and DTT. At the same time, the importance of BSM and the CBT-MEP monitoring looks unshakable in the real-world surgery because real-time feedback brought by ongoing ION procedures plays an indispensable role for the neurosurgeon. In addition, positive and negative BSM results can tell which direction the cortical myelotomy would be safely extended on the surface of the brainstem [81]. Combined application of the latest image-oriented neuronavigation and ION procedures seems indispensable, enabling safer than ever brainstem surgery in the future.

### ***2.7.2 Monitoring of the Reflex Circuit of the Lower Cranial Nerve***

Monitoring of the lower cranial nerve functional integrity is not straightforward. Most of the lower cranial nerve function is composed of reflex circuits, such as gag reflex. Injury to the sensory pathway would produce disturbed lower cranial nerve function.

The CBT-MEP of the laryngeal muscle closely relates to vocalization, which can be traced back to the end of the 1980s when Amassian first demonstrated it by transcranial magnetic stimulation [82]. Clinical application of the laryngeal muscle CBT-MEP monitoring has been reported since then, but non about the neurophysiological monitoring of the functional integrity of reflex circuits of the lower cranial nerves [43, 58]. Further evolution of ION in this field is awaited [83–85].

### ***2.7.3 Stereotactic Biopsy of Brainstem Lesions and the Role of ION***

The paradigm shift is going on in managing diffuse intrinsic pontine glioma (DIPG). The first impact came in the early 1990s when MRI was introduced to diagnose DIPG. Once diagnosed on MRI, DIPGs have been regarded as no surgical indication since then [86]. It should be reminded that Albright did not deny all biopsy surgery for brainstem gliomas. He mentioned the need for biopsy surgeries in 10–15% of brainstem gliomas with atypical MRI findings. Despite his detailed description, the treatment modality of the MRI diagnosis followed by radiation therapy stayed the mainstream of DIPG treatment, with a median survival of less than a year or so for the last two decades [86–88].

The second impact hits at around 2010 when the role of biopsy surgeries was reevaluated because inconsistency of MRI diagnosis of certain DIPGs appeared to be acknowledged [89]. As histopathological heterogenesis of DIPG became more recognized with the advancement of molecular diagnosis, a biopsy surgery has emerged again as an indispensable procedure for the subsequent management of DIPG [90–99]. Direct open biopsy with the use of BSM is desirable in selected cases [93, 96]. On the other hand, less invasive stereotactic biopsy has become a mainstream surgical procedure [100–102]. Presently, convection-enhanced delivery (CED) has appeared in the limelight as a promising new treatment to break through the dilemma of DIPG management [90, 103–106]. Again, stereotactic insertion of a drug-delivering catheter with or without tumor biopsy is required for CED.

Any complications in the brainstem surgery could be severe damage to the patient and should be avoided. The reliability and safety of stereotactic biopsy seem acceptable. Diagnostic success was around 96%, morbidity was 7–8%, with permanent morbidity accounting for 1–2%, and mortality rates less than 1% have been reported [107, 108]. The role of ION in stereotactic brainstem biopsy has not been established yet. However, the combined application of ION of BSM and the white matter mapping could be a useful adjunct for the safe stereotactic brainstem surgery [109, 110]. Figure 2.20 shows an example of a modified application of BSM (stereotactic BSM) for a 59-year-old patient with a brainstem tumor. A specially ordered stimulation electrode whose tip was uninsulated only 1/4 surface for the direction-guide was inserted into a target point of biopsy. Electrical stimulation was delivered to circumscribed structures in all directions at the target. Biopsy samples were obtained from the direction that demonstrated negative mapping. The patient awoke without neurological deterioration, and the pathology of the tumor was malignant lymphoma. A recent paper reported a similar application of BSM during stereotactic biopsy of brainstem lesions in nine patients [111]. The authors utilized a stimulating probe which was integrated into a biopsy needle. Before the biopsy the targeted site was electrically stimulated, and EMG response from CNMNs (VII, IX/X, XII) and the muscles from extremities were monitored. The result sounds intriguing because a targeted biopsy site was modified based on the evoked EMG potentials after electrical stimulation in two out of nine cases. No postoperative

## Stereotactic BSM

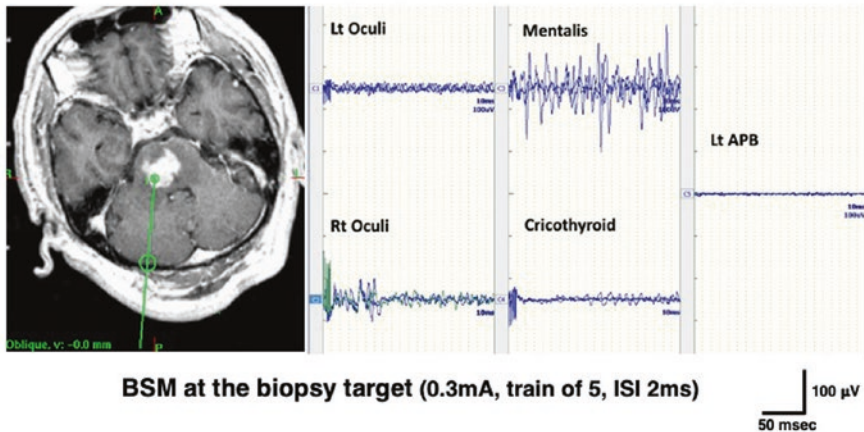


**Fig. 2.20** BSM during a stereotactic brainstem biopsy (stereotactic BSM). Left: BSM was carried out at the target point in a pontine tumor. Right: Positive mapping from the right orbicularis oculi muscle was recorded when the stimulation of BSM was directed at a lateral side of the target point. Biopsy specimens were sampled from the medial side of the target point

complication developed in all patients. This new application of BSM for the stereotactic biopsy of brainstem lesions seems a promising future ION procedure. Less invasive surgery with more sophisticated ION procedures would bring safer than ever brainstem surgery possible.

## 2.8 Summary

The present status and recent advancement of ION in brainstem surgery were reviewed. Special attention was focused on BSM and the CBT-MEP monitoring. The original idea of BSM on the floor of the fourth ventricle was expanded to the wider definition of BSM on the surface of the brainstem. Negative mapping has a clinical role in that the mapped site suggested a safe entry zone to the brainstem. The modern ION procedure can reveal the brainstem's functional surgical anatomy and contribute to the safe brainstem surgery.

The evolution of ION procedures in brainstem surgery are still going on while surgery of the brainstem is advancing with the introduction of skull base approaches and the use of the latest MRI. However, surgery in and around the brainstem still remains a challenge to surgeons even in the era of modern neurosurgery. Image-guided neurosurgery can lead surgeons to reach the brainstem lesion very accurately. However, only ION procedures can reveal distorted functional surgical anatomy on the brainstem and enable monitoring of the functional integrity of CMNs and the motor pathway. Functionally guided brainstem surgery based on the

ION procedures is the critical armamentarium to perform such complex surgery safely. It seems clear that integrated intraoperative application of mapping and monitoring techniques provides the best chance of success in the brainstem surgery. Further development of ION in the stereotactic biopsy of intrinsic brainstem lesions is awaiting.

## References

1. Bricolo A, Turazzi S. Surgery for gliomas and other mass lesions of the brainstem. *Adv Tech Stand Neurosurg.* 1995;22:261–341.
2. Bricolo A. Surgical management of intrinsic brain stem gliomas. *Oper Tech Neurosurg.* 2000;3:137–54.
3. Epstein F. A staging system for brain stem gliomas. *Cancer.* 1985;56:1804–6.
4. Epstein F, McCleary EL. Intrinsic brain-stem tumors of childhood: surgical indications. *J Neurosurg.* 1986;64:11–5.
5. Hoffman JH, Becker L, Craven MA. A clinically and pathologically distinct group of benign brain stem gliomas. *Neurosurgery.* 1980;7:243–8.
6. Bertalanffy H, Ichimura S, Kar S, Tsuji Y, Huang C. Optimal access route for pontine cavernous malformation resection with preservation of abducent and facial nerve function. *J Neurosurg.* 2021;135:683–92.
7. Jallo GI, Biser-Rohrbaugh A, Freed D. Brainstem gliomas. *Childs Nerv Syst.* 2004;20:143–53.
8. Weisenburg TH. Extensive gliomatous tumor involving the cerebellum and the posterior portions of the medulla, pons and cerebral peduncle and the posterior limb of one internal capsule. *J Am Med Assoc.* 1909;53(25):2086–91.
9. Zenner P. Two cases of tumor of the pons. *J Nerv Ment Dis.* 1910;37:27–36.
10. Dmetrichuk JM, Pendleton C, Jallo GI, Quiñones-Hinojosa A. Father of neurosurgery: Harvey Cushing's early experience with a pediatric brainstem glioma at the Johns Hopkins Hospital. *J Neurosurg Pediatr.* 2011;8:337–41.
11. Matson D. Gliomas of the brain stem. In: Matson D, editor. *Neurosurgery of infancy and childhood.* 2nd ed. Springfield, IL: Charles C Thomas; 1969. p. 469–77.
12. Pool JL. Gliomas in the region of the brain stem. *J Neurosurg.* 1968;29:164–7.
13. Pollack IF, Hoffman HJ, Humphreys RP, Becker L. The long-term outcome after surgical treatment of dorsally exophytic brainstem gliomas. *J Neurosurg.* 1993;29:164–7.
14. Stroink AR, Hoffman HJ, Hendrick EB, Humphreys RP, Davidson G. Transependymal benign dorsally exophytic brain stem gliomas in childhood: diagnosis and treatment recommendations. *Neurosurgery.* 1987;20:439–44.
15. Kyoshima K, Kobayashi S, Gibo H, Kuroyanagi T. A study of safe entry zones via the floor of the fourth ventricle for brain-stem lesions: report of three cases. *J Neurosurg.* 1993;78:987–93.
16. Morota N, Deletis V, Epstein FJ, Kofler M, Abbott R, Lee M, Ruskin K. Brain stem mapping: neurophysiological localization of motor nuclei on the floor of the fourth ventricle. *Neurosurgery.* 1995;37:922–30.
17. Morota N, Deletis V, Epstein FJ. Brainstem mapping. In: Deletis V, Shils JL, editors. *Neurophysiology in neurosurgery.* Academic Press: London; 2002. p. 319–35.
18. Strauss C, Lutjen-Drecoll E, Fahlbusch R. Pericolicular surgical approaches to the rhomboid fossa. Part I. Anatomical basis. *J Neurosurg.* 1997;87:893–9.
19. Strauss C, Romstock J, Fahlbusch R. Pericolicular approaches to the rhomboid fossa. Part II. Neurophysiological basis. *J Neurosurg.* 1999;91:768–75.
20. Wiedemayer H, Fauser B, Sandalcioğlu IE, Schäfer H, Stolke D. The impact of neurophysiological intraoperative monitoring on surgical decisions: a critical analysis of 43 cases. *J Neurosurg.* 2002;96:255–62.

21. Fahlbusch R, Strauss C. The surgical significance of brainstem cavernous hemangiomas. *Zentrabl Neurochi.* 1991;52:25–32.
22. Katsuta T, Morioka T, Fujii K, Fului M. Physiological localization of the facial colliculus during direct surgery on an intrinsic brain stem lesion. *Neurosurgery.* 1993;32:861–3.
23. Strauss C, Romstock J, Nimsky C, Fahlbusch R. Intraoperative identification of motor areas of the rhomboid fossa using direct stimulation. *J Neurosurg.* 1993;79:393–9.
24. Morota N, Ihara S, Deletis V. Intraoperative neurophysiology for surgery in and around the brainstem: role of brainstem mapping and corticobulbar tract motor-evoked potential monitoring. *Childs Nerv Syst.* 2010;26:513–21.
25. Sala F, Coppola A, Tramontano V. Intraoperative neurophysiology in posterior fossa tumor in children. *Childs Nerv Syst.* 2015;31:1791–806.
26. Deletis V, Sala F, Morota N. Intraoperative neurophysiological monitoring and mapping during brainstem surgery. A modern approach. *Oper Tech Neurosurg.* 2000;3:109–13.
27. Morota N, Deletis V. The importance of brainstem mapping in brainstem surgical anatomy before the fourth ventricle and implication for intraoperative neurophysiological mapping. *Acta Neurochir.* 2006;148:499–509.
28. Morota N, Deletis V, Epstein F. Brain stem mapping. In: Deletis V, Shils JL, Sala F, Seidel K, editors. *Neurophysiology in neurosurgery.* London: Academic Press; 2020. p. 151–62.
29. Sala F, Manganotti P, Tramontano V, Bricolo A, Gerosa M. Monitoring of motor pathways during brain stem surgery: what we have achieved and what we still miss? *Clin Neurophysiol.* 2007;37:399–406.
30. Tanaka S, Kobayashi I, Utsuki S, Iwamoto K, Takanashi J. Biopsy of brain stem glioma using motor-evoked potential mapping by direct peduncular stimulation and individual adjuvant therapy. *Neuro Med Chir (Tokyo).* 2005;45:49–55.
31. Tanaka S, Takanashi J, Fujii K, Ujiie H, Hori T. Motor evoked potential mapping and monitoring by direct brainstem stimulation. *J Neurosurg.* 2007;107:1053–7.
32. Deletis V, Fernández-Conejero I. Intraoperative monitoring and mapping of the functional integrity of the brainstem. *J Clin Neurol.* 2016;12:262–73.
33. Deletis V. Evoked potential. In: Lake CL, editor. *Clinical monitoring for anesthesia and critical care.* 2nd ed. Philadelphia: W.B. Saunders Co.; 1994. p. 282–314.
34. Cavalheiro S, Yagmurlu K, Silva da Costa MD, Nicácio JM, Rodrigues TP, Chaddad-Neto F, Rhoton AL. Surgical approaches for brainstem tumors in pediatric patient. *Childs Nerv Syst.* 2015;31:1815–40.
35. Mussi AC, Matushita H, Andrade FG, Rhoton AL. Surgical approaches to IV ventricle – anatomical study. *Childs Nerv Syst.* 2015;31:1807–14.
36. Yagmurlu K, Rhoton AL, Tanriover N, Bennett JA. Three-dimensional microsurgical anatomy and the safe entry zones of the brainstem. *Neurosurgery.* 2014;10:602–20.
37. Bogucki J, Czernicki Z, Gielecki J. Cytoarchitectonic basis for safe entry into the brainstem. *Acta Neurochir (Wien).* 2000;142:383–7.
38. Cavalcanti DD, Preul MC, Kalani YS, Spetzler RF. Microsurgical anatomy of safe entry zones to the brainstem. *J Neurosurg.* 2016;124:1359–76.
39. Ferroli P, Schiariti M, Cordella R, Boffano C, Mava S, La Corte E, Cavallo C, Bauer D, Castiglione M, Broggi M, Acerbi F, Broggi G. The lateral infratrigeminal transpontine window to deep pontine lesions. *J Neurosurg.* 2015;123:699–710.
40. Bertalanffy H, Tissira N, Kraysenbühl N, Bozinov O, Sarnthein J. Inter- and inpatient variability of facial nerve response areas in the floor of the fourth ventricle. *Neurosurgery.* 2011;68(ONS Suppl 1):ons23–31.
41. Morota N, Deletis V, Lee M, Epstein FJ. Functional anatomic relationship between brain stem tumors and cranial motor nuclei. *Neurosurgery.* 1996;39:787–94.
42. Schmitt WR, Daube JR, Carlson ML, Mandrekar JN, Beatty CW, Neff B, Driscoll CL, Link MJ. Use of supramaximal stimulation to predict facial nerve outcomes following vestibular schwannoma microsurgery: results from a decade of experience. *J Neurosurg.* 2013;118:206–12.

43. Deletis V, Fernández-Conejero I, Ulkatan S, Rogić M, Carbó EL, Hiltzik D. Methodology for intra-operative recording of the corticobulbar motor evoked potentials from cricothyroid muscles. *Clin Neurophysiol.* 2011;122:1883–9.
44. Sekiya T, Hatayama T, Shimamura N, Suzuki S. Intraoperative electrophysiological monitoring of oculomotor nuclei and their intramedullary tracts during midbrain tumor surgery. *Neurosurgery.* 2000;47:1170–7.
45. Sala F, D'Amico A. Intraoperative neurophysiological monitoring during brainstem surgery. In: Jallo GI, Noureldine MHA, Shimony N, editors. *Brainstem tumors.* Cham: Springer; 2020. p. 109–30.
46. Krieg WJS. *Brain mechanisms in diachrome.* 2nd ed. Bloomington, IL: Brain Books; 1957. p. 287–90.
47. Urban PP, Wicht S, Vucorevic G, Fitzek S, Marx J, Thomke F, Mika-Gruttner A, Fitzek C, Stoeter P, Hopf HC. The course of corticofacial projection in the human brainstem. *Brain.* 2001;124:1866–76.
48. Liégeois FJ, Butler J, Morgan AT, Clayden JD, Clark CA. Anatomy and lateralization of the human corticobulbar tracts: an fMRI-guided tractography study. *Brain Struct Funct.* 2016;221:3337–45.
49. Yim SH, Kim JH, Han ZA, Jeon S, Cho JH, Kim GS, Choi SA, Lee JH. Distribution of the corticobulbar tract in the internal capsule. *J Neurol Sci.* 2013;334:63–8.
50. Terao S, Miura N, Takeda A, Takahashi A, Mitsuma T, Sobue G. Course and distribution of facial corticobulbar tract fibers in the lower brain stem. *J Neuron Neurosurg Psychiatry.* 2000;69:262–5.
51. Oswald AM, Urban NN. There and back again: the corticobulbar loop. *Neuron.* 2012;76:1045–7.
52. Jenabi M, Peck KK, Young RJ, Brennan YN, Holodny AI. Identification of the corticobulbar tracts of the tongue and face using deterministic and probabilistic DTI fiber tracking in patients with brain tumor. *AJNR Am J Neuroradiol.* 2015;36:2036–41.
53. Kanbayashi T, Sonoo M. The course of facial corticobulbar tract fibers in the dorsolateral medulla oblongata. *BMC Neurol.* 2021;21:214.
54. Deletis V, Fernandez-Conejero I, Ulkatan S, Costantino P. Methodology for intraoperatively elicited motor evoked potentials in the vocal muscles by electrical stimulation of the corticobulbar tract. *Clin Neurophysiol.* 2009;120:336–41.
55. Dong CCJ, MacDonald DB, Akagawa R, Westerberg B, Alkhani A, Kanaan I, Hassounah M. Intraoperative facial motor evoked potential monitoring with transcranial electrical stimulation during skull base surgery. *Clin Neurophysiol.* 2005;116:588–96.
56. Fukuda M, Oishi M, Takao T, Saito A, Fujii Y. Facial nerve motor-evoked potential monitoring during skull base surgery predicts facial nerve outcome. *J Neurol Neurosurg Psychiatry.* 2008;79:1066–70.
57. Fukuda M, Oishi M, Hiraishi T, Saito A, Fujii Y. Pharyngeal motor evoked potentials elicited by transcranial electrical stimulation for intraoperative monitoring during skull base surgery. *J Neurosurg.* 2012;116:605–10.
58. Ito E, Ichikawa M, Itakura T, Ando H, Matsumoto Y, Oda K, Sato T, Watanabe T, Sakuma J, Saito K. Motor evoked potential monitoring of the vagus nerve with transcranial electrical stimulation during skull base surgeries. *J Neurosurg.* 2013;118:195–201.
59. Zhang M, Zhou Q, Zhang L, Jiang Y. Facial corticobulbar motor-evoked potential monitoring during the clipping of large and giant aneurysms of the anterior circulation. *J Clin Neurosci.* 2013;20:873–8.
60. Téllez MJ, Ulkatan S, Urriza J, Arranz-Arranz B, Deletis V. Neurophysiological mechanism of possibly confounding peripheral activation of the facial nerve during corticobulbar tract monitoring. *Clin Neurophysiol.* 2016;127:1710–6.
61. Gläsker S, Pechstein U, Vougioukas VI, van Velthoven V. Monitoring motor function during resection of tumours in the lower brain stem and fourth ventricle. *Childs Nerv Syst.* 2006;22:1288–95.

62. Guberinic A, van den Elshout R, Kozicz T, ter Laan M, Hanssen D. Overview of the micro-anatomy of the human brainstem in relation to the safe entry zones. *J Neurosurg.* 2022; 1–11. <https://doi.org/10.3171/2022.2.JNS211997>.
63. Li Z, Wang M, Zhang L, Fan X, Tao X, Qi L, Ling M, Xiao X, Wu Y, Guo D, Qiao H. Neuronavigation-guided corticospinal tract mapping in brainstem tumor surgery: better preservation of motor function. *World Neurosurg.* 2018;116:e291–7.
64. Kamada K, Todo T, Ota T, Ino K, Matsutani Y, Aoki S, Takeuchi F, Kawai K, Saito N. The motor-evoked potential evaluation by tractography and electrical stimulation. *J Neurosurg.* 2009;111:785–95.
65. Shibani E, Krieg SM, Haller B, Buchmann N, Obermueller T, Boeckh-Behrens T, Wostrack M, Meyer B, Ringel F. Intraoperative subcortical motor evoked potential stimulation: how close is the corticospinal tract? *J Neurosurg.* 2015;123:711–20.
66. Nossek E, Korn A, Shahar T, Kanner AA, Yaffe H, Marcovici D, Ben-Harosh C, Ami HB, Weinstein M, Shapira-Lichter I, Constantini S, Hendler T, Ram Z. Intraoperative mapping and monitoring of the corticospinal tracts with neurophysiological assessment and 3 dimensional ultrasonography-based navigation. *J Neurosurg.* 2011;114:738–46.
67. Yamaguchi F, Ten H, Higuchi T, Omura T, Kojima T, Adachi K, Kitamura T, Kobayashi S, Takahashi H, Teramoto A, Morita A. An intraoperative motor tract positioning method in brain tumor surgery: technical note. *J Neurosurg.* 2018;129:576–82.
68. Deshmukh VR, Rangel-Castilla L, Spetzler RF. Lateral inferior cerebellar peduncle approach to dorsolateral medullary cavernous malformation. *J Neurosurg.* 2014;121:723–9.
69. Šteňo J, Bízík I, Šteňová J, Timárová G. Subtemporal transtentorial resection of cavernous malformations involving the pyramidal tract in the upper pons and mesencephalon. *Acta Neurochir.* 2011;153:1955–62.
70. Da L, Hao SY, Tang J, Xiao XR, Jia GJ, Wu Z, Zang LW, Zhang JT. Surgical management of pediatric brainstem cavernous malformations. *J Neurosurg Pediatr.* 2014;13:484–502.
71. Gross BA, Batjer HH, Awad IA, Bendok BR. Brainstem cavernous malformations. *Neurosurgery.* 2009;64:805–18.
72. Niemann K, van den Boom R, Haeselbarth K, Afshar F. A brainstem stereotactic atlas in a three-dimensional magnetic resonance imaging navigation system: first experiences with atlas-to-patient registration. *J Neurosurg.* 1999;90:891–901.
73. Berman JI, Berger MS, Chung SW, Nagarajan SS, Henry RG. Accuracy of diffusion tensor magnetic resonance imaging tractography assessed using intraoperative subcortical stimulation mapping and magnetic source imaging. *J Neurosurg.* 2007;107:488–94.
74. Ohue S, Kohno S, Inoue A, Yamashita D, Harada H, Kumon Y, Kikuchi K, Miki H, Ohnishi T. Accuracy of diffusion tensor magnetic resonance imaging-based tractography for surgery of gliomas near the pyramidal tract: a significant correlation between subcortical electrical stimulation and postoperative tractography. *Neurosurgery.* 2012;70:283–94.
75. Czernicki T, Maj E, Podgórska A, Kunert P, Prokopienko M, Nowak A, Cieszanowski A, Marchel A. Diffusion tensor tractography of pyramidal tracts in patients with brainstem and intramedullary spinal cord tumors: relationship with motor deficits and intraoperative MEP changes. *J Magn Reson Imaging.* 2017;46:715–23.
76. Ille S, Schroeder A, Wagner A, Negwer C, Kreiser K, Meyer B, Krieg SM. Intraoperative MRI-based elastic fusion for anatomically accurate tractography of the corticospinal tract: correlation with intraoperative neuromonitoring and clinical status. *Neurosurg Focus.* 2021;50(1):E9.
77. Mikuni N, Okada T, Nishida N, Taki J, Enatsu R, Ikeda A, Miki Y, Hanakawa T, Fukuyama H, Hashimoto N. Comparison between motor evoked potential recording and fiber tracking for estimating pyramidal tracts near brain tumors. *J Neurosurg.* 2007;106:128–33.
78. Flores BC, Whittemore AR, Samson DS, Barnett S. The utility of preoperative diffusion tensor imaging in the surgical management of brainstem cavernous malformation. *J Neurosurg.* 2015;122:653–62.

79. Xiao X, Kong L, Pan C, Zhang P, Chen X, Sun T, Wang M, Qiao H, Wu Z, Zhang J, Zhang L. The role of diffusion tensor imaging and tractography in the surgical management of brainstem gliomas. *Neurosurg Focus*. 2021;50(1):E10.
80. Rusheen AE, Goyal A, Owen RL, Berning EM, Bothun DT, Giblon RE, Blaha CD, Welker KM, Hustn J III, Bennet KE, Oh Y, Fagan AJ, Lee KH. The development of ultra-high field MRI guidance technology for neuronavigation. *J Neurosurg*. 2022; 1–13. <https://doi.org/10.3171/2021.11.JNS211078>.
81. Kalani MYS, Yagmurlu K, Martirosyan NL, Cavalcanti DD, Spetzler RF. Approach selection for intrinsic brainstem pathologies. *J Neurosurg*. 2016;125:1596–607.
82. Amassian VE, Anziska BJ, Cracco JB, Cracco RQ, Maccabee PJ. Focal magnetic excitation of frontal cortex activates laryngeal muscles in man. *Proc Physiol Soc*. 1987; 41.
83. Téllez MJ, Ulkatan S, Sinclair CF. Intraoperative monitoring of the vagus and laryngeal nerves with the laryngeal adductor reflex. In: Deletis V, Shils JL, Sala F, Seidel K, editors. *Neurophysiology in neurosurgery. A modern approach*. 2nd ed. London: Academic press; 2020. p. 209–21.
84. Téllez MJ, Ulkatan S. Bringing the masseter reflex into the operating room. In: Deletis V, Shils JL, Sala F, Seidel K, editors. *Neurophysiology in neurosurgery. A modern approach*. 2nd ed. London: Academic press; 2020. p. 223–8.
85. Fernández-Conejero I, Deletis V. Blink reflex. In: Deletis V, Shils JL, Sala F, Seidel K, editors. *Neurophysiology in neurosurgery. A modern approach*. 2nd ed. London: Academic press; 2020. p. 229–37.
86. Albright AL, Packer RJ, Zimmerman R, Rorke LB, Boyett J, Hammond GD. Magnetic resonance scans should replace biopsies for the diagnosis of diffuse brain stem gliomas: a report from the Children’s Cancer Group. *Neurosurgery*. 1993;33:1026–9.
87. Farmer JP, Montes JL, Freeman CR, Meagher-Villemure K, Bond MC, O’Gorman AM. Brainstem gliomas: a 10-year institutional review. *Pediatr Neurosurg*. 2001;34:206–14.
88. Rechberger JS, Lu VM, Zhang L, Power EA, Daniels DJ. Clinical trials for diffuse intrinsic pontine glioma: the current state of affairs. *Childs Nerv Syst*. 2020;36:39–46.
89. Hankinson TC, Campagna EJ, Foreman NK, Handler MH. Interpretation of magnetic resonance images in diffuse intrinsic pontine glioma: a survey of pediatric neurosurgeons. *J Neurosurg Pediatr*. 2011;8:97–102.
90. Frazier JL, Lee J, Thomale UW, Noggle JC, Cohen K, Jallo GI. Treatment of diffuse intrinsic brainstem gliomas: failed approaches and future strategies. *J Neurosurg Pediatr*. 2009;3:259–69.
91. Hersh DS, Kumar R, Moore KA, Smith LGF, Tinkle CL, Chiang J, Patay Z, Gajjar A, Choudhri AF, Lee-Diaz J, Vaughn B, Klimo P. Safety and efficacy of brainstem biopsy in children and young adults. *J Neurosurg Pediatr*. 2020;26:552–62.
92. Dellaretti M, Touzet G, Reyns N, Dubois F, Gusmão S, Pereira JLB, Blond S. Correlation among magnetic resonance imaging findings, prognostic factors for survival, and histological diagnosis of intrinsic brainstem lesions in children. *J Neurosurg Pediatr*. 2011;8:539–43.
93. Sufit A, Donson AM, Birks DK, Knipstein JA, Fenton LZ, Jedlicka P, Hankinson TC, Handler MH, Foreman NK. Diffuse intrinsic pontine tumors: a study of primitive neuroectodermal tumors versus more common diffuse intrinsic pontine gliomas. *J Neurosurg Pediatr*. 2012;10:81–8.
94. Phi JH, Chung HT, Wang KC, Ryu SK, Kim SK. Transcerebellar biopsy of diffuse pontine gliomas in children: a technical note. *Childs Nerv Syst*. 2013;29:489–93.
95. Cage TA, Samagh SP, Mueller S, Nicolaides T, Haas-Kogan D, Prados M, Banerjee A, Auguste KI, Gupta N. Feasibility, safety, and indications for surgical biopsy of intrinsic brainstem tumors in children. *Childs Nerv Syst*. 2013;29:1313–9.
96. Ogiwara H, Morota N. The efficacy of a biopsy of intrinsic brainstem lesions for decision making of the treatments. *Childs Nerv Syst*. 2013;29:833–7.
97. Pincus DW, Richter EO, Yachnis AT, Bennett J, Bhatti T, Smith A. Brainstem stereotactic biopsy sampling in children. *J Neurosurg*. 2006;104(2 Suppl):108–14.

98. Rajshekhar V, Moorthy RK. Status of stereotactic biopsy in children with brain stem masses: insights from a series of 106 patients. *Stereotact Funct Neurosurg.* 2010;88:360–6.
99. Samadani U, Judy KD. Stereotactic brainstem biopsy is indicated for the diagnosis of a vast array of brainstem pathology. *Stereotact Funct Neurosurg.* 2003;81:5–9.
100. Puget S, Beccaria K, Blauwblomme T, Roujeau T, James S, Grill J, Zerah M, Varlet P, Sainte-Rose C. Biopsy in series of 130 pediatric diffuse intrinsic pontine gliomas. *Childs Nerv Syst.* 2015;31:1773–80.
101. Williams JR, Young CC, Vidanza NA, McGrath M, Feroze AH, Browd SR, Hauptman JS. Progress in diffuse intrinsic pontine glioma: advocating for stereotactic biopsy in the standard of care. *Neurosurg Focus.* 2020;48(1):E4.
102. Jaradat A, Nowacki A, Fishtner J, Schlaeppli JA, Pollo C. Stereotactic biopsies of brainstem lesions: which approach? *Acta Neurochir.* 2021;163:1957–64.
103. Anderson RCE, Kennedy B, Yanes CL, Garvin J, Needle M, Canoll P, Feldstein NA, Bruce JN. Convection-enhanced delivery of topotecan into diffuse intrinsic brainstem tumors in children. *J Neurosurg Pediatr.* 2013;11:289–95.
104. Chittiboina P, Heiss JD, Warren KE, Lonser RR. Magnetic resonance imaging properties of convective delivery in diffuse intrinsic pontine gliomas. *J Neurosurg Pediatr.* 2014;13:276–82.
105. Kuzan-Fischer CM, Souweidane MM. The intersect of neurosurgery with diffuse intrinsic pontine glioma. *J Neurosurg Pediatr.* 2019;24:611–21.
106. Souweidane MM, Kramer K, Pandit-Taskar N, Zhou Z, Haque S, Zanzonico P, Carrasquillo JA, Lyashchenko SK, Thakur SB, Donzelli M, Turner RS, Lewis JS, Cheung NKV, Larson SM, Dunkel IJ. Convection-enhanced delivery for diffuse intrinsic pontine glioma: a single-center, dose-escalation, phase 1 trial. *Lancet Oncol.* 2018;19:1040–50.
107. Hamisch C, Kickingereder P, Fischer M, Simon T, Ruge MI. Update on the diagnostic value and safety of stereotactic biopsy for pediatric brainstem tumors: a systematic review and meta-analysis of 735 cases. *J Neurosurg Pediatr.* 2017;20:261–8.
108. Kickingereder P, Willet P, Simon T, Ruge MI. Diagnostic value and safety of stereotactic biopsy for brainstem tumors: a systematic review and meta-analysis of 1480 cases. *Neurosurgery.* 2013;72:873–82.
109. Iijima K, Hirato M, Miyagishima T, Horiguchi K, Sugawara K, Hirato J, Yokoo H, Yoshimoto Y. Microrecording and image-guided stereotactic biopsy of deep-seated brain tumors. *J Neurosurg.* 2015;123:978–88.
110. Ooba H, Abe T, Momii Y, Fujiki M. Stereotactic biopsy with electrical monitoring for deep-seated brain tumors. *World Neurosurg.* 2013;79(207):e1–201.e5.
111. Labuschagne J, Mutyaba D, Nel J, Casieri C. Use of intra-operative stimulation of brainstem lesion target sites for frameless stereotactic biopsies. *Childs Nerv Syst.* 2021;37:1515–23.